




Group 1 metabotropic glutamate receptors trigger glutamate-induced intracellular Ca^{2+} signals and nitric oxide release in human brain microvascular endothelial cells

Sharon Negri¹ · Pawan Faris^{1,2} · Giorgia Pellavio³ · Laura Botta¹ · Matteo Orgiu¹ · Greta Forcaia⁴ · Giulio Sancini⁴ · Umberto Laforenza³ · Francesco Moccia¹ 

Received: 21 March 2019 / Revised: 2 August 2019 / Accepted: 16 August 2019 / Published online: 31 August 2019
© Springer Nature Switzerland AG 2019

Abstract

Neurovascular coupling (NVC) is the mechanism whereby an increase in neuronal activity causes an increase in local cerebral blood flow (CBF) to ensure local supply of oxygen and nutrients to the activated areas. The excitatory neurotransmitter glutamate gates post-synaptic *N*-methyl-D-aspartate receptors to mediate extracellular Ca^{2+} entry and stimulate neuronal nitric oxide (NO) synthase to release NO, thereby triggering NVC. Recent work suggested that endothelial Ca^{2+} signals could underpin NVC by recruiting the endothelial NO synthase. For instance, acetylcholine induced intracellular Ca^{2+} signals followed by NO release by activating muscarinic 5 receptors in hCMEC/D3 cells, a widely employed model of human brain microvascular endothelial cells. Herein, we sought to assess whether also glutamate elicits metabotropic Ca^{2+} signals and NO release in hCMEC/D3 cells. Glutamate induced a dose-dependent increase in intracellular Ca^{2+} concentration ($[\text{Ca}^{2+}]_i$) that was blocked by α -methyl-4-carboxyphenylglycine and phenocopied by *trans*-1-amino-1,3-cyclopentanedicarboxylic acid, which, respectively, block and activate group 1 metabotropic glutamate receptors (mGluRs). Accordingly, hCMEC/D3 expressed both mGluR1 and mGluR5 and the Ca^{2+} response to glutamate was inhibited by their pharmacological blockade with, respectively, CPCOEt and MTEP hydrochloride. The Ca^{2+} response to glutamate was initiated by endogenous Ca^{2+} release from the endoplasmic reticulum and endolysosomal Ca^{2+} store through inositol-1,4,5-trisphosphate receptors and two-pore channels, respectively, and sustained by store-operated Ca^{2+} entry. In addition, glutamate induced robust NO release that was suppressed by pharmacological blockade of the accompanying increase in $[\text{Ca}^{2+}]_i$. These data demonstrate for the first time that glutamate may induce metabotropic Ca^{2+} signals in human brain microvascular endothelial cells. The Ca^{2+} response to glutamate is likely to support NVC during neuronal activity, thereby reinforcing the emerging role of brain microvascular endothelial cells in the regulation of CBF.

Keywords Glutamate · Neurovascular coupling · Brain microvascular endothelial cells · Group 1 metabotropic glutamate receptors · Ca^{2+} signaling · Nitric oxide

Electronic supplementary material The online version of this article (<https://doi.org/10.1007/s00018-019-03284-1>) contains supplementary material, which is available to authorized users.

✉ Francesco Moccia
francesco.moccia@unipv.it

¹ Laboratory of General Physiology, Department of Biology and Biotechnology “Lazzaro Spallanzani”, University of Pavia, Via Forlanini 6, 27100 Pavia, Italy

² Research Center, Salahaddin University, Erbil, Kurdistan-Region of Iraq, Iraq

³ Human Physiology Unit, Department of Molecular Medicine, University of Pavia, Pavia, Italy

⁴ Department of Experimental Medicine, University of Milano-Bicocca, Monza, Italy

Introduction

Lying at the interface between circulation and vascular tissues, the endothelium serves as a signal transduction platform that integrates hemodynamic forces and blood-borne signals to regulate multiple vascular processes, including vascular tone and permeability as well as vascular structure [1–4]. Appropriate control of local blood flow through resistance arteries is critical to ensure the proper supply of oxygen and nutrients, as well as the removal of catabolic waste, and to maintain blood pressure within the physiological range [5, 6]. Vascular endothelial cells respond to vasodilatory autacoids by releasing diffusible mediators, such as nitric oxide (NO) and prostacyclin (PGI₂), and/or by undergoing membrane hyperpolarization that spreads to medial smooth muscle cells via myoendothelial gap junctions (MEGJs) to suppress contractility, according to a mechanism termed endothelium-dependent hyperpolarization (EDH) [3, 7, 8]. An increase in endothelial intracellular Ca²⁺ concentration ([Ca²⁺]_i) represents the signal which recruits the most effective vasorelaxing pathways in the vascular wall [3, 7, 9]. For instance, endothelial Ca²⁺ signals stimulate NO release by engaging the Ca²⁺-dependent calmodulin (CaM) to displace endothelial nitric oxide (NO) synthase (eNOS) from caveolin-1, whereas PGI₂ is synthesized by cyclooxygenase which acts on the arachidonic acid cleaved from membrane phospholipids by the Ca²⁺-dependent phospholipase A₂ (PLA₂) [3, 8].

Physiologically, extracellular autacoids bind to their cognate G_q-protein-coupled receptors (G_qPCRs), thereby stimulating phospholipase Cβ (PLCβ) to cleave phosphatidylinositol 4,5-bisphosphate (PIP₂), a minor (≈ 1%) membrane phospholipid, into the intracellular second messengers, inositol-1,4,5-trisphosphate (InsP₃) and diacylglycerol (DAG) [2, 4]. InsP₃, in turn, elicits massive Ca²⁺ release from the endoplasmic reticulum (ER) through InsP₃ receptors (InsP₃Rs), followed by Ca²⁺ influx via a store-operated Ca²⁺ entry (SOCE) pathway on the plasma membrane [9, 10]. Endothelial SOCE is mainly mediated by the physical interaction between STIM1, a sensor of ER Ca²⁺ concentration, and Orai1, which provides the pore-forming subunit of store-operated channels [11, 12]. Vascular endothelial cells also express the STIM and Orai paralogues, STIM2, Orai2, and Orai3 [11, 13, 14]. STIM2 is likely to trigger SOCE in STIM1-deficient endothelial cells [14], whereas Orai2 acts as a negative modulator of Orai1 [15], as recently demonstrated in other cell types [16, 17]. In addition, endogenous Ca²⁺ release may be supported by endolysosomal Ca²⁺ release through nicotinic acid adenine dinucleotide phosphate (NAADP)-gated two-pore channels 1 and 2 (TPC1-2), which trigger InsP₃-induced ER

Ca²⁺ mobilization through the Ca²⁺-induced Ca²⁺ release (CICR) process in response to extracellular stimulation [14, 18]. Endothelial Ca²⁺ signals control the vascular tone by driving NO release in response to a multitude of autacoids, including acetylcholine [19, 20], ATP [21], bradykinin [22], histamine [23], and thrombin [24], throughout peripheral circulation. Surprisingly, endothelial Ca²⁺ signaling has barely been regarded as an active participant in neurovascular coupling (NVC) [8, 25, 26], the mechanism by which neuronal activity induces vasorelaxation of cortical microvessels to redirect cerebral blood flow (CBF) to activated areas [27, 28].

NVC is crucial to maintain the homeostasis of the brain internal milieu and to sustain normal brain function; moreover, several vascular-based functional brain imaging techniques, such as functional magnetic resonance imaging (fMRI), rely on NVC to infer changes in neuronal activity [27–29]. Glutamate, the major excitatory neurotransmitter in the brain, triggers NVC by stimulating post-synaptic *N*-methyl-D-aspartate (NMDA) receptors (NMDARs) to mediate extracellular Ca²⁺ entry, thereby engaging the Ca²⁺/CaM-dependent neuronal NOS (nNOS) [27, 28, 30]. NO may directly stimulate vasorelaxation of adjacent microvessels in hippocampus and cerebellum [31, 32], while it permits the vasodilatory response to astrocyte-derived vasoactive mediators, such as epoxyeicosatrienoic acids (EETs) and prostaglandin E₂ (PGE₂), in the somato-sensory cortex [33–38]. Pharmacological blockade of group 1 metabotropic glutamate receptors (mGluRs), i.e., mGluR1 and mGluR5, which are G_qPCRs coupled to PLCβ and InsP₃-dependent Ca²⁺ release, also attenuates the hemodynamic response to sensory stimulation in vivo [39–42]. The earlier model according to which mGluRs were mainly located in perisynaptic astrocytes was later discounted by the discovery that mGluR5 downregulates to barely detectable levels in adult astrocytes and that the genetic deletion of type 2 InsP₃R, the principal InsP₃R isoform in glial cells, does not inhibit NVC [43–45]. Therefore, the exact mechanism whereby group 1 mGluRs control NVC remains unclear [27, 46]. Conversely, group 2 mGluRs include the mGluR2 and mGluR3, which are G_{i/o} coupled receptors and inhibit adenylate cyclase (AC). Finally, group 3 mGluRs comprise mGluR4, mGluR7, and mGluR8, which are also negatively coupled to AC, and mGluR6, which stimulates a cGMP phosphodiesterase [47]. Group 2 and group 3 mGluRs mainly exhibit a pre-synaptic location and inhibit neurotransmitter (glutamate or GABA) release [47]. Therefore, their role in NVC is less clear.

Intriguingly, a series of recent studies demonstrated that synaptically released glutamate could induce NO release directly from brain microvascular endothelial cells [48]. For instance, glutamate has been shown to elicit NO release within rodent brain microvasculature by activating endothelial NMDARs in cortical microvessels [49, 50] and

group 1 mGluRs in mouse brain microvascular endothelial cells [51]. These results strongly support the observation that long-term synaptic plasticity requires endothelial-derived NO at the Schaffer collateral to CA1 synapse in mouse hippocampal slices [52], and that synaptic glutamate induces vascular NO release in response to whisker stimulation in the somato-sensory cortex in vivo [48]. It has recently been demonstrated that acetylcholine generates an intracellular Ca^{2+} signal which drives NO release in hCMEC/D3 cells, a widely employed human brain microvascular endothelial cell line [53]. Acetylcholine-induced NO synthesis was initiated by endogenous Ca^{2+} release through type 3 InsP_3R ($\text{InsP}_3\text{R}3$) and endolysosomal TPC1-2, was sustained by SOCE [53], and triggered a robust hemodynamic response in the somato-sensory cortex in vivo [48]. Early investigations reported that mGluR1 and mGluR5 are expressed in human brain microvascular cells [54] and in human meningeal microvasculature, as well as in the parenchymal microvasculature [55], but their functional role remains unclear.

Herein, we exploited a multidisciplinary approach to assess whether and how group 1 mGluRs induce Ca^{2+} -dependent NO release in hCMEC/D3 cells. We provided the evidence that glutamate causes a dose-dependent increase in $[\text{Ca}^{2+}]_i$ by activating mGluR1 and, at a larger extent, mGluR5. Glutamate-induced Ca^{2+} signal is supported by InsP_3 - and NAADP-dependent intracellular Ca^{2+} release and is prolonged by SOCE. Finally, the metabotropic Ca^{2+} response to glutamate leads to rapid NO release, which is abolished by inhibition of endogenous Ca^{2+} release. These findings reinforce the emerging view that brain microvascular endothelial cells may be recruited by neuronal activity to control NVC.

Materials and methods

Cell culture

Human brain endothelial cells (hCMEC/D3) were obtained from Institut National de la Santé et de la Recherche Médicale (INSERM, Paris, France). hCMEC/D3 cells cultured between passage 25 and 35 were used. As described in [53], the cells were seeded at a concentration of 27,000 cells/cm² and grown in tissue culture flasks coated with 0.1 mg/mL rat tail collagen type 1, in the following medium: EBM-2 medium (Lonza, Basel, Switzerland) supplemented with 5% fetal bovine serum (FBS), 1% Penicillin–Streptomycin, 1.4 μM hydrocortisone, 5 $\mu\text{g}/\text{mL}$ ascorbic acid, 1/100 chemically defined lipid concentrate (Invitrogen), 10 mM HEPES, and 1 ng/mL basic FGF (bFGF). The cells were cultured at 37 °C, 5% CO_2 saturated humidity.

Solutions

Physiological salt solution (PSS) had the following composition (in mM): 150 NaCl, 6 KCl, 1.5 CaCl_2 , 1 MgCl_2 , 10 Glucose, 10 Hepes. In Ca^{2+} -free solution (0Ca^{2+}), Ca^{2+} was substituted with 2 mM NaCl, and 0.5 mM EGTA was added. Solutions were titrated to pH 7.4 with NaOH. In Mn^{2+} -quenching experiments, 200 μM MnCl_2 was added to the 0Ca^{2+} external solution. The osmolality of PSS as measured with an osmometer (Wescor 5500, Logan, UT) was 338 mmol/kg.

$[\text{Ca}^{2+}]_i$ and NO measurements

We utilized the Ca^{2+} imaging set-up that we have described elsewhere [56]. hCMEC/D3 cells were loaded with 4 μM fura-2 acetoxymethyl ester (Fura-2/AM; 1 mM stock in dimethyl sulfoxide) in PSS for 1 h min at 37 °C and 5% CO_2 . After washing in PSS, the coverslip was fixed to the bottom of a Petri dish and the cells observed by an upright epifluorescence Axiolab microscope (Carl Zeiss, Oberkochen, Germany), usually equipped with a Zeiss $\times 40$ Achroplan objective (water immersion, 2.0 mm working distance, 0.9 numerical aperture). The cells were excited alternately at 340 and 380 nm, and the emitted light was detected at 510 nm. A first neutral density filter (1 or 0.3 optical density) reduced the overall intensity of the excitation light and a second neutral density filter (optical density = 0.3) was coupled to the 380 nm filter to approach the intensity of the 340 nm light. A round diaphragm was used to increase the contrast. The excitation filters were mounted on a filter wheel (Lambda 10, Sutter Instrument, Novato, CA, USA). Custom software, working in the LINUX environment, was used to drive the camera (Extended-ISIS Camera, Photonic Science, Millham, UK) and the filter wheel, and to measure and plot on-line the fluorescence from 30 to 45 rectangular “regions of interest” (ROI) enclosing 20–30 single cells. Each ROI was identified by a number. Adjacent ROIs never superimposed. $[\text{Ca}^{2+}]_i$ was monitored by measuring, for each ROI, the ratio of the mean fluorescence emitted at 510 nm when exciting alternatively at 340 and 380 nm [ratio (F_{340}/F_{380})]. An increase in $[\text{Ca}^{2+}]_i$ causes an increase in the ratio [14]. Ratio measurements were performed and plotted on-line every 3 s. The experiments were performed at room temperature (22 °C) [57].

NO was measured as described in [53]. Briefly, hCMEC/D3 cells were loaded with the membrane-permeable NO-sensitive dye 4-Amino-5-methylamino-2',7'-difluorofluorescein (DAF-FM) diacetate (10 μM) for 60 min at room temperature and washed in PSS for 15 min. DAF-FM fluorescence was measured using the same equipment described for Ca^{2+} recordings but with a different filter set, i.e., excitation at 480 nm and emission at 535 nm wavelength (emission

intensity was shortly termed “NO_i”). The changes in DAF-FM fluorescence induced by glutamate were recorded and plotted on-line every 5 s. Again, off-line analysis was performed using custom-made macros developed by Microsoft Office Excel software. The experiments were performed at room temperature (22 °C). DAF-FM fluorescence remained constant during 1 h recording at the sampling rate and light intensity employed in the present investigation (not shown).

RNA isolation and real-time RT-PCR (qRT-PCR)

Total RNA was extracted from hCMEC/D3 cells using the QIAzol Lysis Reagent (QIAGEN, Italy). Reverse transcription and qRT-PCR were performed as previously described [14] using specific primers (intron-spanning primers). The specific intron-spanning primers and the molecular weight of the amplicon (in parentheses) were indicated below: mGluR1, sense, 5'-GTCCACACGGAAGGGAATTATG-3'; antisense, 5'-GAGTTTGCGCAAGAGTCGGT-3' (144 bp); mGluR5, sense, 5'-GCACACAGAAGGCAACTA TG-3'; antisense, 5'-TTGGGCAAGTGACTTGTGAG-3' (159 bp); B2 M, Hs_B2M_1_SG QuantiTect Primer Assay QT00088935 (Qiagen, Italia) (98 bp).

The qRT-PCR reactions were normalized using β -2-microglobulin (B2 M) as housekeeping gene. The triplicate threshold cycle (C_t) values for each sample were averaged resulting in mean C_t values for both the gene of interest and the housekeeping genes. The gene C_t values were then normalized to the housekeeping gene by taking the difference: $\Delta C_t = C_t[\text{gene}] - C_t[\text{housekeeping}]$, with high ΔC_t values reflecting low mRNA expression levels. Melting curves were generated to detect the melting temperatures of specific products immediately after the PCR run. The molecular weight of the PCR products was compared to the DNA molecular weight marker VIII (Roche Molecular Biochemicals, Italy).

Immunoblotting

Cells were homogenized using a Dounce homogenizer in a solution containing: 250 mM Sucrose, 1 mM EDTA, 10 mM Tris-HCl, pH 7.6, 0.1 mg/ml PMSF, 100 mM β -mercaptoethanol, protease, and phosphatase inhibitor cocktails (P8340 and P5726, P0044, Sigma-Aldrich Inc.). 30 μ g of solubilized proteins were subjected to 7.5% SDS-polyacrylamide gel electrophoresis and blotted to the Hybond-P PVDF Membrane (GE Healthcare, Italy). Membranes were blocked for 1 h with Tris-buffered saline (TBS) containing 3% BSA and 0.1% Tween (blocking solution) and then incubated overnight at 4 °C with the following antibodies diluted in the TBS and 0.1% Tween: anti-mGluR1 (AGC-006; 1: 200, dilution), anti-mGluR5 (AGC-007; 1:200, dilution) from Alomone labs, Jerusalem BioPark

(JBP), Jerusalem, Israel. After 3 washing with TBS and 0.1% Tween, membranes were incubated for 1 h with goat anti-rabbit IgG antibody, peroxidase conjugated (API32P, Millipore part of Merck S.p.a., Vimodrone, Italy), diluted 1:10,000 in blocking solution. The bands were detected with ECLTM Select western blotting detection system (GE Healthcare Europe GmbH, Italy). Prestained molecular weight markers (ab116028, Abcam, Cambridge, UK) were used to estimate the molecular weight of the bands. Blots were stripped with the method of Yeung and Stanley [58] and re-probed with anti β -2-microglobulin antibody (B2 M) (Abcam) as housekeeping. The antibody was diluted 1:10,000 in blocking solution.

Protein content

Protein contents of all the samples were determined by the Bradford's method [59] using bovine serum albumin (BSA) as standard.

Statistics

All the data have been collected from hCMEC/D3 cells deriving from at least three coverslips from three independent experiments. The amplitude of Ca²⁺ and NO signals induced by each agonist was measured as the difference between the ratio at the peak of intracellular Ca²⁺ mobilization and the mean ratio of 1 min baseline before the peak. Pooled data are given as mean \pm SE and statistical significance ($P < 0.05$) was evaluated by the Student's *t* test for unpaired observations as indicated. Data are presented as mean \pm SE, while the number of cells analysed is indicated within/above the histogram bars.

Chemicals

Fura-2/AM and DAF-FM were obtained from Molecular Probes (Molecular Probes Europe BV, Leiden, The Netherlands). (RS)- α -methyl-4-carboxyphenylglycine (MCPG) was supplied by Abcam Biochemicals (Cambridge, UK). CPC-COEt, MTEP hydrochloride (MTEP), CHPG, YM-58483/BTP-2, and NED-19 were purchased from Tocris (Bristol, UK). All the chemicals were of analytical grade and obtained from Sigma Chemical Co. (St. Louis, MO, USA).

Results

Glutamate induces a dose-dependent increase in [Ca²⁺]_i in hCMEC/D3 cells

To assess whether glutamate induces intracellular Ca²⁺ signals, hCMEC/D3 cells were loaded with the Ca²⁺-sensitive

fluorochrome, Fura-2/AM, as shown in [53]. Unlike bEND5 cells, a mouse brain microvascular endothelial cell line [51], hCMEC/D3 did not exhibit any spontaneous Ca²⁺ activity in the absence of external stimulation (data not shown). The extracellular application of glutamate induced a discernible increase in [Ca²⁺]_i, which consisted in an initial Ca²⁺ peak followed by a plateau level of intermediate amplitude above resting [Ca²⁺]_i (Fig. 1a). Thereafter, the Ca²⁺ signal declined to the baseline despite for the continuous presence of the agonist in the bath (Fig. 1a). Glutamate (100 μM) failed to induce an additional increase in [Ca²⁺]_i upon 15 min wash-out (Fig. 1d), which is indicative of receptor desensitization. The percentage of responding cells did not significantly change throughout the concentration range that we probed (Fig. 1a, b), i.e., 50–300 μM, but the peak Ca²⁺ response was attained at 100 μM as the Ca²⁺ signal desensitized at higher doses (Fig. 1a, c). Overall, these data demonstrate for the first time that glutamate is able to increase the [Ca²⁺]_i in a human model of brain microvascular endothelial cells at physiological doses [60, 61]. As 100 μM proved to be the most effective dose to induce the glutamate-evoked Ca²⁺ signal, we employed this concentration throughout the remainder of the investigation.

mGluR1 and mGluR5 trigger the Ca²⁺ response to glutamate in hCMEC/D3 cells

The Ca²⁺ response to glutamate described in Fig. 1 was recorded in the absence of extracellular glycine or D-serine, which unmask endothelial NMDAR activation in mouse middle cerebral arteries [49, 50]. Group 1 mGluRs represent, therefore, the most suitable target for glutamate to induce Ca²⁺ signaling in hCMEC/D3 cells. To corroborate this hypothesis, we first challenged hCMEC/D3 cells with glutamate (100 μM) in the absence of extracellular Ca²⁺ (0Ca²⁺). As shown in Fig. 2a–c, removal of extracellular Ca²⁺ did not affect the initial Ca²⁺ peak, as it would be expected in the case of NMDAR activation [62], although it curtailed the duration of the Ca²⁺ response. This finding strongly suggests that glutamate-evoked Ca²⁺ signals are initiated by group 1 mGluRs, which are coupled to G_q and able to engage PLCβ, thereby inducing InsP₃-dependent Ca²⁺ release from the ER [47, 63]. The subsequent re-addition of extracellular Ca²⁺, in the absence of glutamate to prevent the opening of receptor-operated channels, resulted in a second increase in [Ca²⁺]_i (Fig. 2b), which was indicative of SOCE recruitment [51, 53, 56]. Accordingly, as glutamate was removed from the

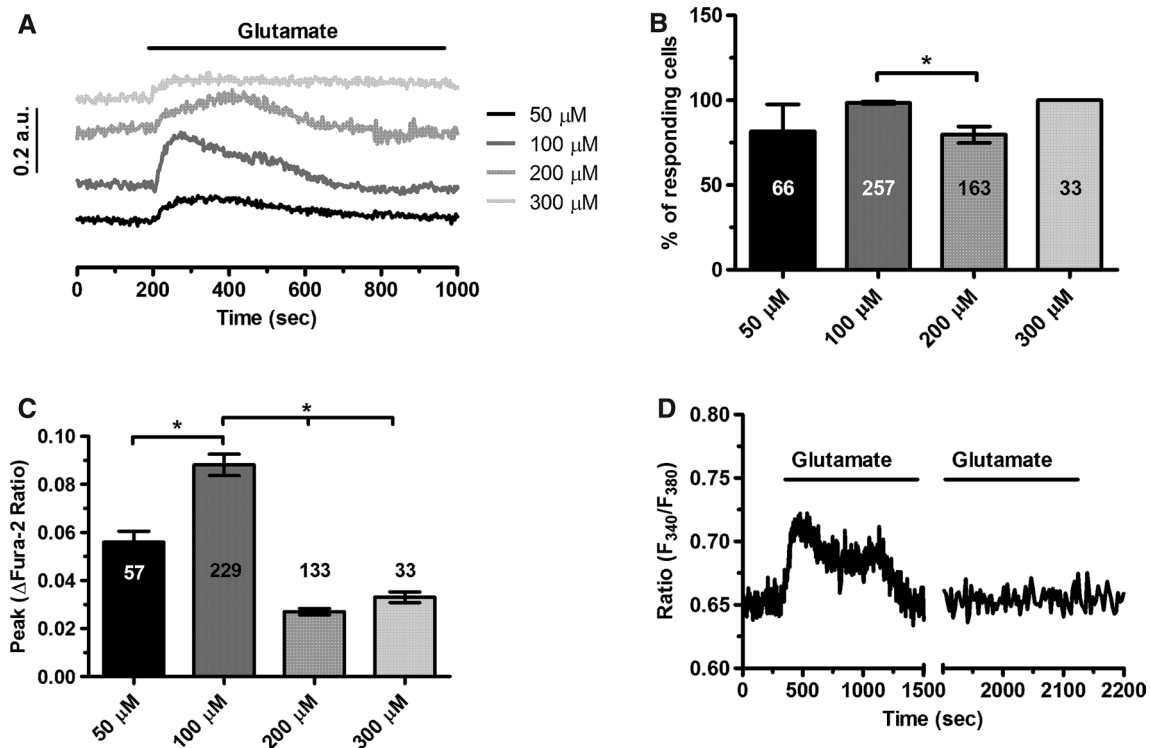


Fig. 1 Glutamate evokes a dose-dependent increase in [Ca²⁺]_i in hCMEC/D3 cells. **a** Glutamate caused a dose-dependent increase in [Ca²⁺]_i which achieved its peak at 100 M. **b** Mean ± SE of the percentage of hCMEC/D3 cells displaying glutamate-induced Ca²⁺ responses at different agonist concentrations (from 50 to 300 μM). The asterisk indicates *p* < 0.05. **c** Mean ± SE of the amplitude of

glutamate-induced Ca²⁺ responses measured in hCMEC/D3 cell at different agonist concentrations (from 50 to 300 μM). The asterisk indicates that *p* < 0.05. **d** Glutamate (100 μM) failed to induce an additional increase in [Ca²⁺]_i upon 15 min washout which is indicative of receptor desensitization

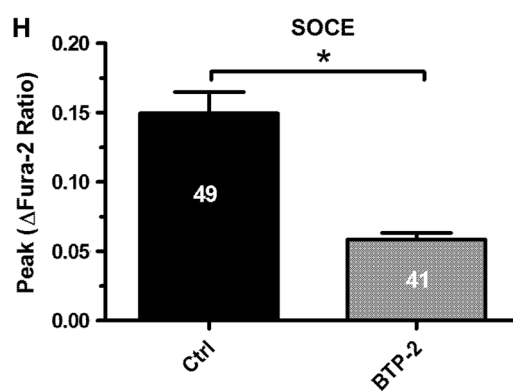
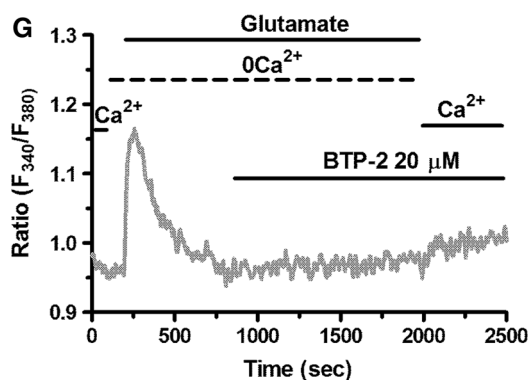
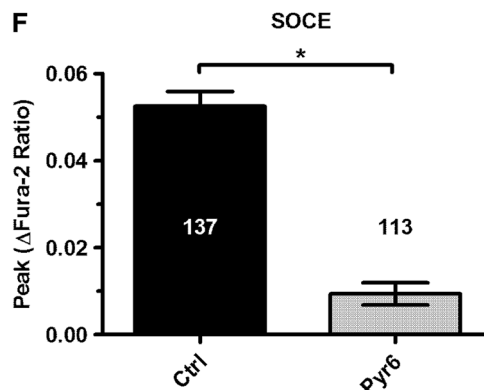
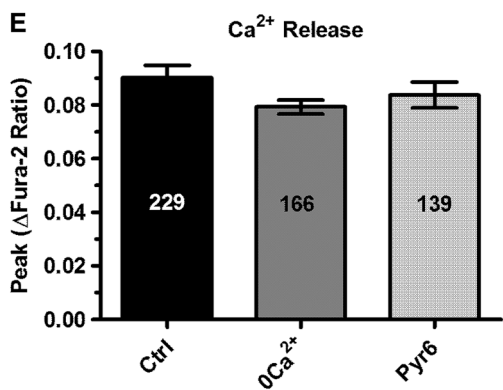
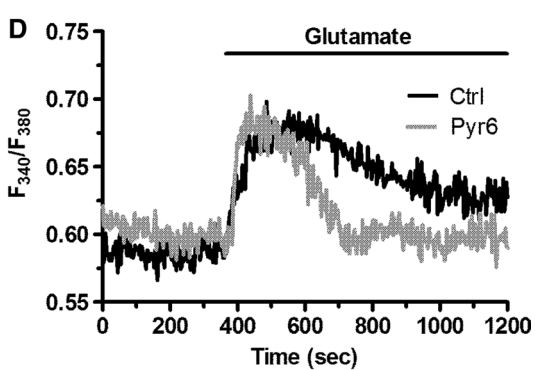
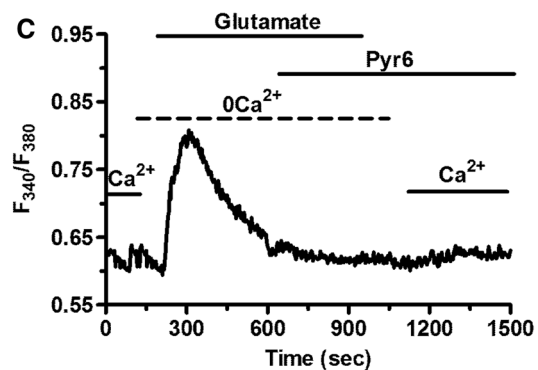
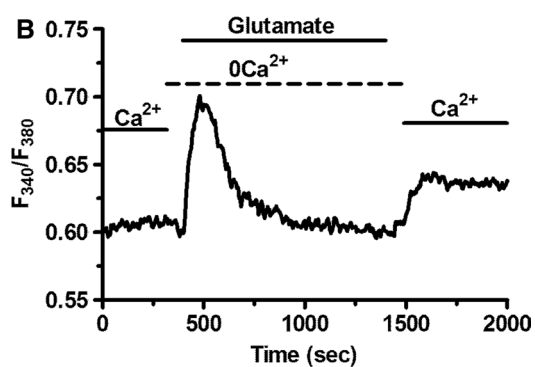
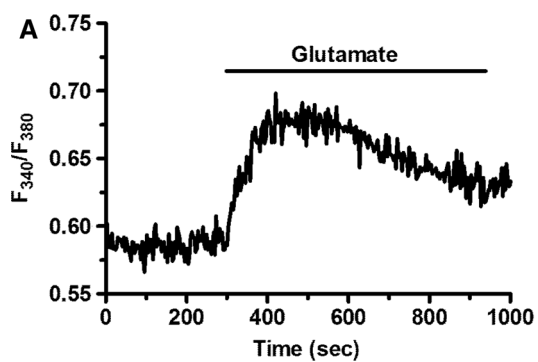


Fig. 2 The Ca²⁺ response to glutamate requires endogenous Ca²⁺ release and Orai1-mediated Ca²⁺ entry. **a** Glutamate (100 μM) induced a biphasic increase in [Ca²⁺]_i in the presence of extracellular Ca²⁺ in hCMEC/D3 cells. **b** Removal of extracellular Ca²⁺ (0Ca²⁺) did not affect the initial Ca²⁺ peak, although it curtailed the duration of the Ca²⁺ response. Restoration of extracellular Ca²⁺ upon removal of glutamate resulted in a second bump in [Ca²⁺]_i, which was indicative of SOCE. **c** Pyr6 (10 μM, 10 min), a selective inhibitor of Orai1, prevented glutamate-induced Ca²⁺ entry in hCMEC/D3 cells. **d** Preincubating the cells with Pyr6 (10 μM, 10 min) did not affect the magnitude of the Ca²⁺ response to glutamate, but curtailed the plateau phase. **e** Bar histogram shows the mean ± SE of the amplitude of the Ca²⁺ release in control (Ctrl) cells, under 0Ca²⁺ condition and upon treatment with Pyr6 (10 μM, 10 min). **f** Bar histogram shows the mean ± SE of SOCE amplitude in control cells and upon treatment with Pyr6 (10 μM, 10 min). **g** BTP-2 (20 μM, 20 min), a selective inhibitor of Orai1, prevented glutamate-induced Ca²⁺ entry in hCMEC/D3 cells. **h** Bar histogram shows the mean ± SE of SOCE amplitude in control (Ctrl) cells and upon treatment with BTP-2 (20 μM, 20 min)

bath 100 s before restoration of extracellular Ca²⁺ levels, the only physiological stimulus responsible for Ca²⁺ entry was ER Ca²⁺ store depletion. As widely discussed elsewhere [64, 65], neither ionotropic receptors, i.e., NMDARs [49, 50], nor second messenger-operated channels, e.g., Transient Receptor Potential (TRP) Vanilloid 4 (TRPV4) [26], can be gated in the absence of agonist binding to their cognate receptors. In addition, hCMEC/D3 cells express very low levels of TRP Canonical 7 (TRPC7) channel, which is gated by DAG [14]. However, 1-oleoyl-2-acetyl-sn-glycerol (OAG), a membrane-permeable analogue of DAG, failed to induce sizeable Ca²⁺ signals in hCMEC/D3 cells [14]. This finding has been confirmed in Supplementary Figure 1A. Collectively, these pieces of evidence strongly support the view that SOCE mediates glutamate-induced extracellular Ca²⁺ entry in hCMEC/D3 cells. A previous report demonstrated that hCMEC/D3 cells express STIM2, but not STIM1, as well as all Orai isoforms. However, SOCE was sensitive to Pyr6 [14], which is a selective Orai1 inhibitor [66–68]. These data, therefore, strongly support the notion that SOCE is mediated by STIM2 and Orai1 in hCMEC/D3 cells. In agreement with this model, glutamate-induced extracellular Ca²⁺ entry was suppressed by Pyr6 (10 μM, 10 min) (Fig. 2c, f). In addition, Pyr6 (10 μM, 10 min) curtailed the Ca²⁺ response to glutamate without affecting the initial peak (Fig. 2d, e), thereby mimicking the Ca²⁺ signal recorded in the absence of extracellular Ca²⁺. To further support the involvement of Orai1 in glutamate-evoked Ca²⁺ entry, we probed the effect of two other specific Orai1 inhibitors, S66 [69, 70] and BTP-2 [69, 71]. Unfortunately, S66 (10 μM) induced intracellular Ca²⁺ oscillations even in the absence of extracellular Ca²⁺ (0Ca²⁺) (Supplementary Figure 2), which might reflect previously unreported off-target effects. Conversely, BTP-2 (10 μM) did not elicit any increase in [Ca²⁺]_i (Supplementary Figure 3B). Our preliminary experiments

confirmed that BTP-2 (10 μM, 20 min) suppressed SOCE induced by previous depletion of the ER Ca²⁺ pool with CPA (10 μM) (Supplementary Figure 3). Furthermore, BTP-2 (10 μM, 20 min) also inhibited glutamate-evoked Ca²⁺ entry (Fig. 2g, h), which reinforces the hypothesis that Orai1 mediates glutamate-dependent SOCE in hCMEC/D3 cells.

Taken together, these results indicate that group 1 mGluRs drive the Ca²⁺ response to glutamate in hCMEC/D3 cells. In agreement with this hypothesis, we next found that glutamate-evoked Ca²⁺ signals were abolished by MCPG (150 μM, 20 min) (Fig. 3a, c, d), a broad-spectrum group 1 mGluR antagonist [32, 51, 62]. Conversely, the Ca²⁺ response to glutamate was phenocopied by *trans*-1-amino-1,3-cyclopentanedicarboxylic acid (*trans*-ACPD or tACPD; 100 μM), a selective agonist of group 1 mGluRs [72] (Fig. 3b–d). In agreement with these observations, Western blot analysis confirmed that both mGluR1 and mGluR5 proteins were broadly expressed in hCMEC/D3 cells. Immunoblots showed a major band of about 150 kDa for both mGluR1 and mGluR5 (Fig. 4a), which is in the size range indicated by the manufacturer. Moreover, qRT-PCR analysis, carried out using the specific primers described in Materials and methods, found that both mGluR1 and mGluR5 transcripts were expressed in hCMEC/D3 cells, although the latter was less abundant (Fig. 4b). In agreement with these recordings, the Ca²⁺ response to glutamate (100 μM) was sensitive to both CPCCOEt (100 μM, 10 min) and MTEP (100 μM, 10 min) (Fig. 4c), which, respectively, block mGluR1 and mGluR5 [39–42]. Accordingly, MTEP significantly (*p* < 0.05) reduced the percentage of responding cells (Fig. 4d, left panel) and the peak Ca²⁺ response (Fig. 4d, right panel), whereas CPCCOEt only attenuated the amplitude of the initial Ca²⁺ peak (Fig. 4d). Notably, the inhibitory effect of MTEP was slightly stronger as compared to CPCCOEt (Fig. 4d, right panel). To confirm the hypothesis that mGluR5 was tightly coupled to intracellular Ca²⁺ signalling in hCMEC/D3 cells, we exploited the selective mGluR5 agonist CHPG [73]. As shown in Supplementary Figure 4, CHPG (25 μM) induced an increase in [Ca²⁺]_i in 65 out of 65 hCMEC/D3 cells. Unfortunately, no specific mGluR1 agonist is available and we could not assess mGluR1 capability to elicit intracellular Ca²⁺ signals in hCMEC/D3 cells. Taken together, these findings demonstrate that mGluR1 and mGluR5 mediate glutamate-evoked Ca²⁺ signals in hCMEC/D3 cells.

The PLCβ/InsP₃ signalling pathway sustains the intracellular Ca²⁺ response to glutamate in hCMEC/D3 cells

As anticipated earlier, glutamate-induced endogenous Ca²⁺ release in the absence of extracellular Ca²⁺ is likely

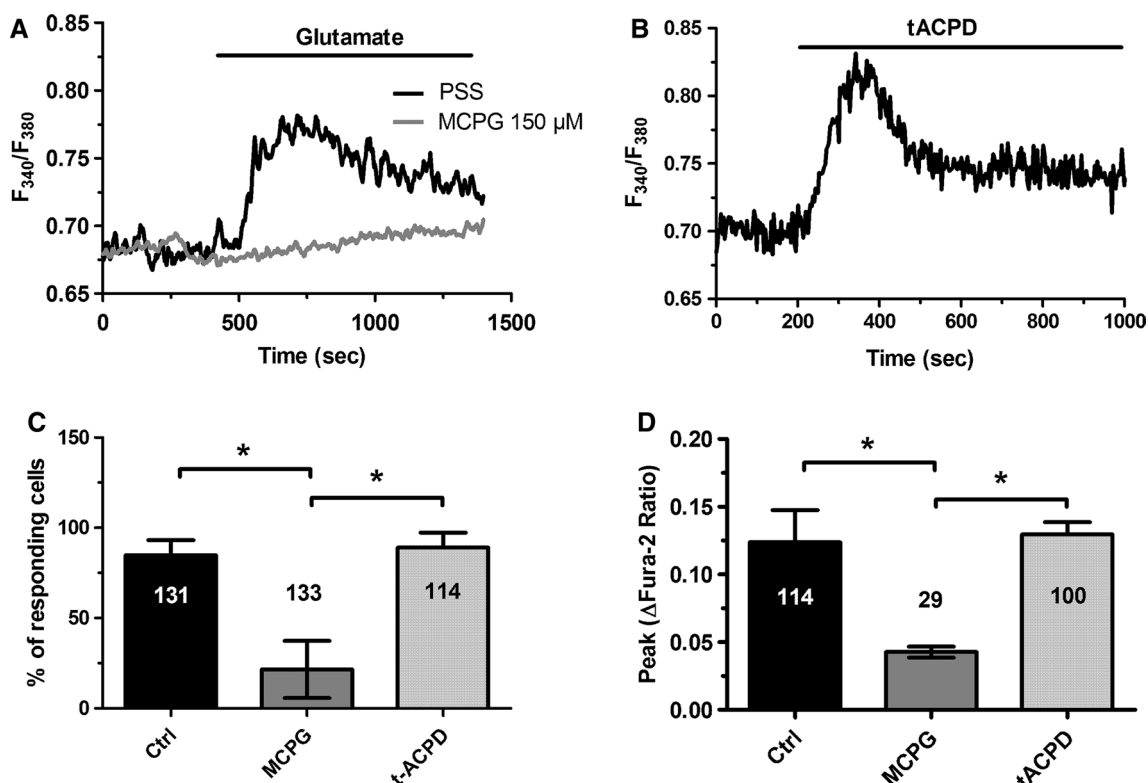


Fig. 3 The Ca^{2+} response to glutamate is mediated by metabotropic glutamate receptors (mGluRs). **a** Glutamate ($100 \mu\text{M}$) caused a rapid increase in $[\text{Ca}^{2+}]_i$, which was inhibited by MCPG ($150 \mu\text{M}$, 20 min), a broad-spectrum group 1 mGluR antagonist. **b** Trans-ACPD ($100 \mu\text{M}$), a selective agonist of group 1 mGluRs, mimicked the Ca^{2+}

response to glutamate. **c** Bar histogram shows the mean \pm SE of the percentage of responding cells under the designated treatments. The asterisk indicates $p < 0.05$. **d** Bar histogram shows the mean \pm SE of the amplitude of the Ca^{2+} response under the designated treatments. The asterisk indicates $p < 0.05$

to be supported by ER-embedded InsP_3Rs , as mGluR1 and mGluR5 are coupled to G_q [47, 63]. In agreement with this hypothesis, the intracellular Ca^{2+} response to glutamate ($100 \mu\text{M}$) was suppressed by U73122 ($10 \mu\text{M}$, 30 min) (Fig. 5a, c, d), an aminosteroid which selectively blocks PLC in brain microvascular endothelial cells [51, 53, 56], and by 2-aminoethoxydiphenyl borate (2-APB; $50 \mu\text{M}$, 30 min), which selectively inhibits InsP_3Rs in the absence of extracellular Ca^{2+} at this concentration [74, 75] (Fig. 5a, c, d). In addition, glutamate-induced endogenous Ca^{2+} release was abrogated by depleting the ER Ca^{2+} store with cyclopiazonic acid (CPA; $10 \mu\text{M}$), which is widely employed to impair Sarco-Endoplasmic Reticulum Ca^{2+} -ATPase (SERCA) activity. As reported elsewhere [53], CPA caused a transient increase in $[\text{Ca}^{2+}]_i$, which was due to passive Ca^{2+} efflux through ER leakage channel followed by Ca^{2+} removal from the cytosol (Fig. 5b). The subsequent addition of glutamate ($100 \mu\text{M}$) failed to induce any detectable elevation in $[\text{Ca}^{2+}]_i$ due to previous emptying of the ER Ca^{2+} store. Taken together, these data confirmed that the PLC β / InsP_3 signalling pathway sustains glutamate-induced endogenous Ca^{2+} release in hCMEC/D3 cells, as suggested by the role of mGluR1 and mGluR5 in the onset of the signal.

NAADP-induced Ca^{2+} mobilization contributes to glutamate-induced intracellular Ca^{2+} release in hCMEC/D3 cells

We recently reported that acetylcholine-induced intracellular Ca^{2+} release in hCMEC/D3 cells was supported by NAADP-dependent EL Ca^{2+} mobilization through TPC1-2 [53]. Likewise, Glycyl-L-phenylalanine 2-naphthylamide (GPN; $200 \mu\text{M}$), a cathepsin C substrate that mobilizes lysosomal Ca^{2+} by osmotic rupture of the acidic vesicles [76, 77], caused a transient increase in $[\text{Ca}^{2+}]_i$ in the absence of extracellular Ca^{2+} (0Ca^{2+}), thereby preventing the subsequent glutamate-induced endogenous Ca^{2+} release (Fig. 6a, c, d). Furthermore, the intracellular Ca^{2+} response to glutamate ($100 \mu\text{M}$) was prevented by NED-19 ($100 \mu\text{M}$, 30 min) (Fig. 6b–d), a selective TPC1-2 antagonist [78, 79]. Collectively, these findings demonstrated that NAADP-gated EL TPC1-2 contribute to glutamate-induced endogenous Ca^{2+} release in hCMEC/D3 cells.

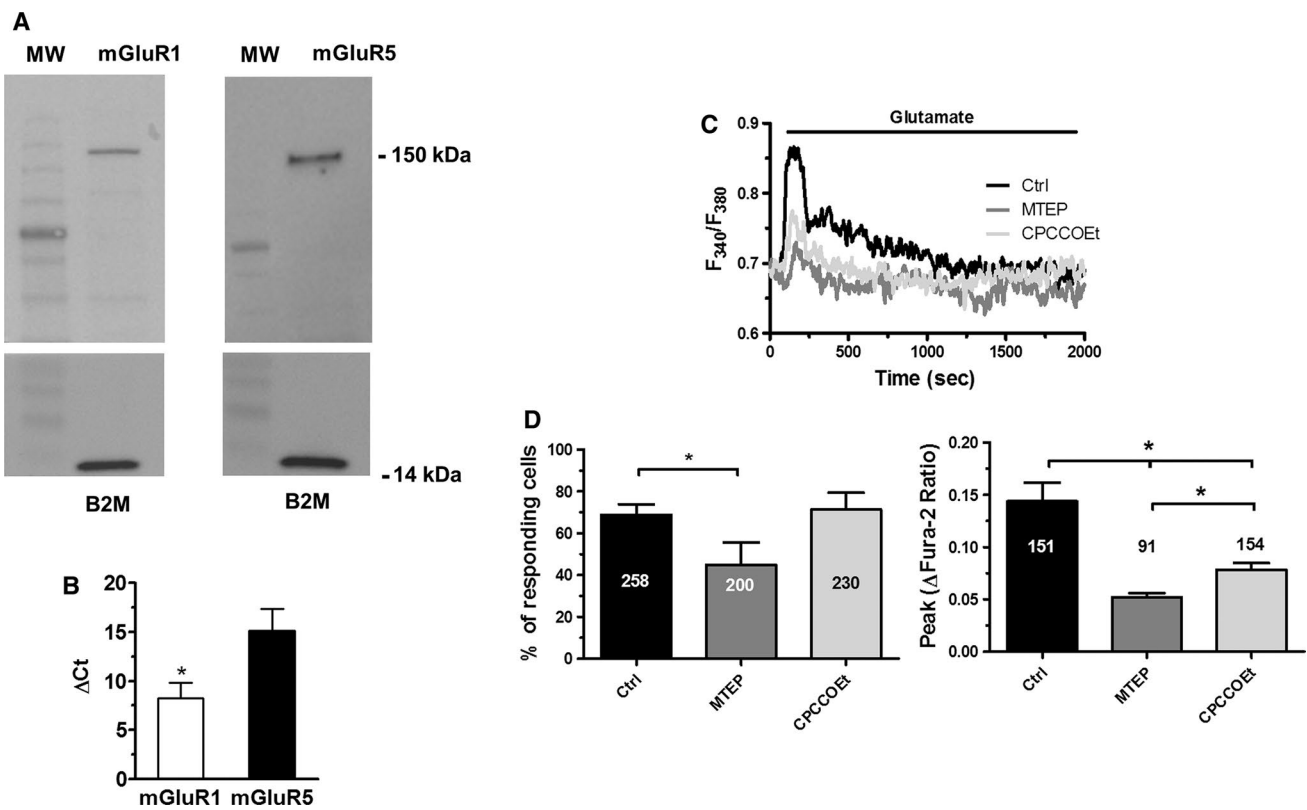


Fig. 4 The Ca²⁺ response to glutamate is mediated by mGluR1 and mGluR5. **a** Expression of mGluR1 and mGluR5 proteins in hCMEC/D3 cells. Blots representative of four independent experiments were shown. Lanes were loaded with 30 μg of proteins, probed with affinity purified antibodies, and processed as described in “Materials and methods”. The same blots were stripped and re-probed with anti-beta-2-microglobulin (B2M) polyclonal antibody, as housekeeping. Major bands of the expected molecular weights were indicated. **b** Expression of mGluR1 and mGluR5 transcripts in hCMEC/D3 cells. Reverse transcription polymerase chain reaction of total RNA

was performed using specific primers as indicated in Materials and methods. **c** Glutamate (100 μM) caused a rapid increase in [Ca²⁺]_i which was reduced by CPCCOEt (100 μM, 10 min) and MTEP (100 μM, 10 min), which, respectively, block mGluR1 and mGluR5. **d** Left panel, bar histogram shows the mean ± SE of the percentage of responding cells in control conditions and upon treatment with MTEP (100 μM, 10 min) and CPCCOEt (100 μM, 10 min). Right panel, bar histogram shows the mean ± SE of the amplitude of the response under the designated treatments. The asterisk indicates that $p < 0.05$

Glutamate-induced intracellular Ca²⁺ signaling drives NO release in hCMEC/D3 cells

To assess whether and how glutamate induces Ca²⁺-dependent NO release, we loaded hCMEC/D3 cells with the NO-sensitive fluorophore, DAF-FM, as described in [53]. Glutamate (100 μM) caused an immediate increase in DAF-FM fluorescence that was inhibited by pretreating the cells with L-NAME (100 μM, 1 h) (Fig. 7a), a widely employed NOS inhibitor, or BAPTA (30 μM, 2 h) (Fig. 7a), a membrane-permeant buffer of intracellular Ca²⁺ levels [51, 53]. Furthermore, glutamate-induced NO release was phenocopied by tACPD (100 μM) (Fig. 7b) and blocked by MCPG (150 μM, 20 min) (Fig. 7c). In further agreement with the Ca²⁺ imaging data, MTEP (100 μM, 10 min) and CPCCOEt (100 μM, 10 min) significantly ($p < 0.05$) reduced NO production in hCMEC/D3 cells challenged with glutamate (Fig. 7d). The statistical analysis of NO release under

each of these conditions is presented in Fig. 7e, f. These data, therefore, demonstrate that mGluR1 and mGluR5 drive NO release by recruiting eNOS in a Ca²⁺-dependent manner also in human brain microvascular endothelial cells.

Subsequently, we found that glutamate-induced NO release occurred also in the absence of extracellular Ca²⁺ (0Ca²⁺), whereas Ca²⁺ restitution to the perfusate did not cause any detectable increase in DAF-FM fluorescence (Fig. 8a). Furthermore, pharmacological blockade of SOCE with Pyr6 (10 μM, 10 min) did not reduce glutamate-induced NO release (Fig. 8b). Likewise, suppressing SOCE with BTP-2 (20 μM, 20 min) did not affect glutamate-induced NO production (Supplementary Figure 5). As expected, OAG failed to increase DAF-FM fluorescence in hCMEC/D3 cells (Supplementary Figure 1B–D). Furthermore, glutamate-induced NO release was not affected by simultaneously blocking SOCE with Pyr6 (10 μM, 10 min) and TRPC7 with La³⁺ (100 μM, 20 min) (Supplementary Figure 6). These

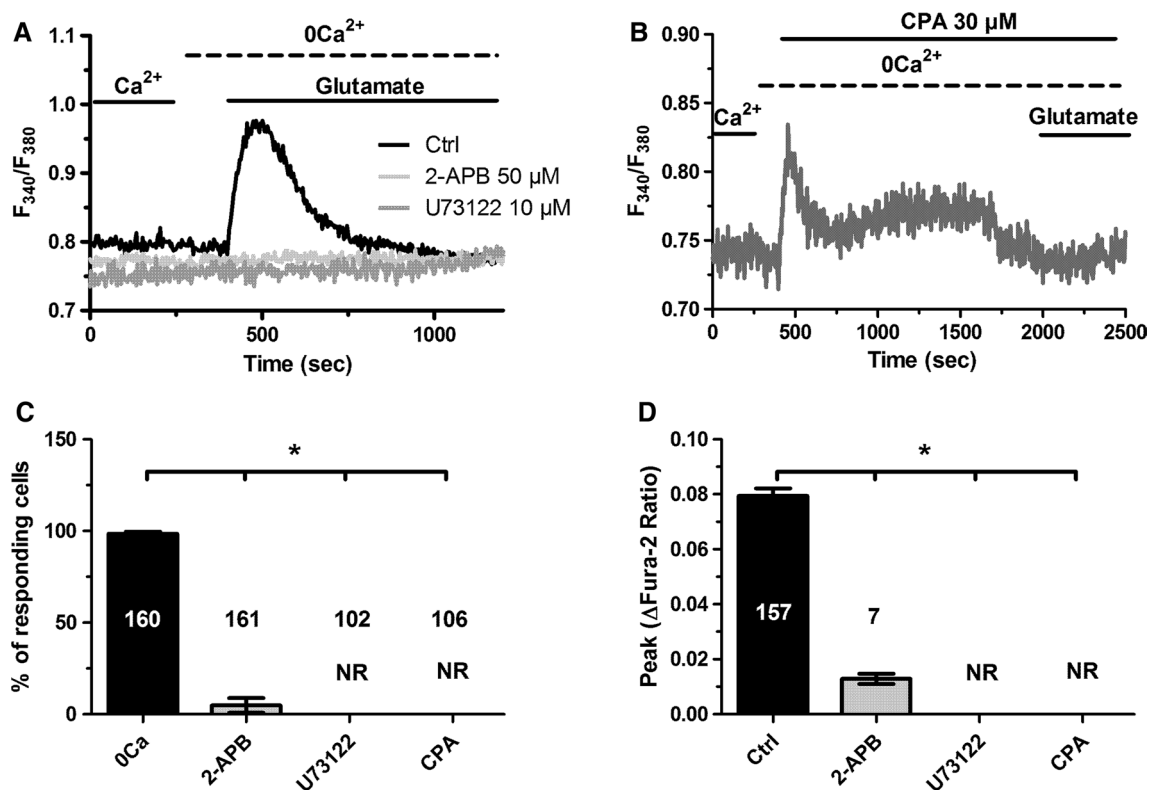


Fig. 5 Glutamate-induced endogenous Ca^{2+} mobilization requires ER-dependent Ca^{2+} release through InsP_3Rs . **a** The Ca^{2+} response to glutamate ($100 \mu\text{M}$) was inhibited by U73122 ($10 \mu\text{M}$, 30 min), a selective PLC blocker. Moreover, the Ca^{2+} signal was inhibited by blocking InsP_3Rs with 2-APB ($50 \mu\text{M}$, 30 min). **b** Emptying the ER Ca^{2+} pool with CPA ($10 \mu\text{M}$), a selective SERCA inhibitor, prevented the Ca^{2+} response to glutamate. As expected, CPA elicited a tran-

sient elevation in $[\text{Ca}^{2+}]_i$ due to the passive depletion of the ER Ca^{2+} pool followed by Ca^{2+} clearing through the plasma membrane and by mitochondria. **c** Bar histogram shows the mean \pm SE of the percentage of responding cells under the designated treatments. The asterisk indicates that $p < 0.05$. **d** Bar histogram shows the mean \pm SE of the amplitude of the Ca^{2+} response under the designated treatments. The asterisk indicates that $p < 0.05$. NR no response

data strongly suggest that glutamate drives NO production through the endogenous Ca^{2+} release. Accordingly, glutamate failed to increase DAF-FM fluorescence in the presence of U73122 ($10 \mu\text{M}$, 30 min) and 2-APB ($50 \mu\text{M}$, 30 min) (Fig. 8c). Moreover, glutamate-induced NO release was abrogated following depletion of the EL Ca^{2+} pool with GPN ($200 \mu\text{M}$, 30 min) (Fig. 8d) and upon pharmacological blockade of TPC1-2 channels with NED-19 ($100 \mu\text{M}$, 30 min) (Fig. 8d). Taken together, these findings demonstrated that InsP_3 and NAADP sustain glutamate-induced NO release in hCMEC/D3 cells. The statistical analysis of these data has been reported in Fig. 8e, f.

Discussion

Herein, we showed for the first time that glutamate induces a transient increase in $[\text{Ca}^{2+}]_i$ in human brain microvascular endothelial cells. The Ca^{2+} response to glutamate is triggered by mGluR1 and mGluR5, initiated by endogenous Ca^{2+} release driven by the Ca^{2+} releasing messengers, InsP_3

and NAADP, and sustained by SOCE. Glutamate-induced intracellular Ca^{2+} signalling, in turn, causes a robust NO release, which could play a key role in the slower component of NVC. These data, therefore, lend further support to the emerging notion that neuronal activity may be sensed by perisynaptic microvessels [38, 42, 49, 80, 81] and that brain microvascular endothelial cells fulfil a crucial function in the hemodynamic response to synaptic activity [8, 29].

mGluR1 and mGluR5 trigger the Ca^{2+} response to glutamate in hCMEC/D3 cells

Early studies demonstrated that group 1 mGluRs mediate glutamate-induced decrease in blood–brain barrier (BBB) permeability by inducing the dephosphorylation of vasodilator-stimulated phosphoprotein (VASP) [54]. Notably, disassembly of adherent junctions between adjacent vascular endothelial cells may also be triggered by endothelial Ca^{2+} signals [82]. A recent investigation demonstrated that glutamate evokes metabotropic Ca^{2+} signals in mouse brain microvascular endothelial cells, thereby resulting in massive

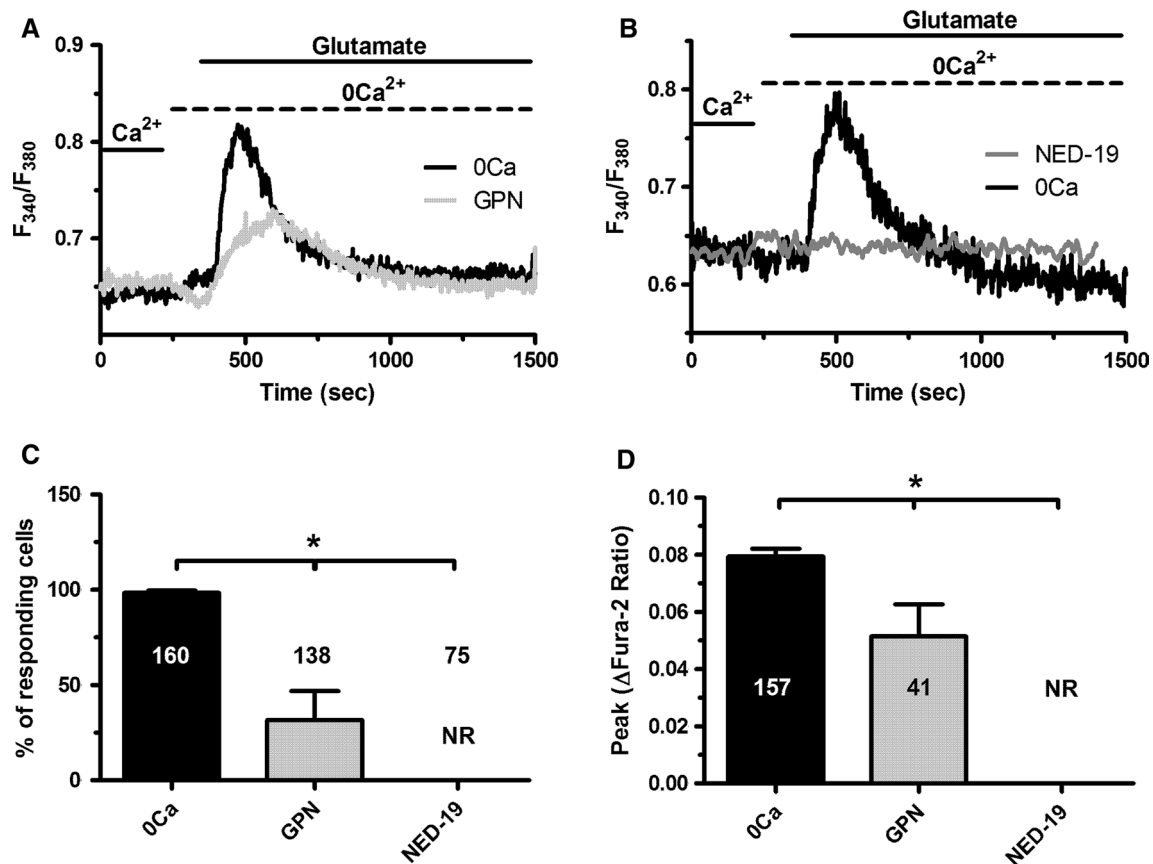


Fig. 6 NAADP-induced intracellular Ca²⁺ mobilization contributes to glutamate-induced endogenous Ca²⁺ release in hCMEC/D3 cells. **a** GPN (200 μM), a lysosomotropic agent that is widely used to deplete the EL Ca²⁺ store, prevented the Ca²⁺ response to glutamate (100 μM). **b** Glutamate-induced increase in [Ca²⁺]_i in the absence, but not in the presence, of NED-19 (100 μM, 30 min), a

selective TPC inhibitor. Glutamate was administered at 100 μM. **c** Bar histogram shows the mean ± SE of the percentage of responding cells under the designated treatments. The asterisk indicates *p* < 0.05. **d** Bar histogram shows the mean ± SE of the amplitude of the Ca²⁺ response under the designated treatments. The asterisk indicates *p* < 0.05. *NR* no response

NO production [51]. Therefore, we decided to assess whether group 1 mGluRs were expressed and able to increase the [Ca²⁺]_i in the human cerebrovascular endothelial cell line hCMEC/D3 [83–86]. Glutamate induced a dose-dependent increase in [Ca²⁺]_i in hCMEC/D3 cells, which attained a peak at 100 μM and consisted in a rapid Ca²⁺ transient which then declined to a plateau level before returning to the baseline. This Ca²⁺ waveform was strikingly different from the repetitive [Ca²⁺]_i oscillations induced by glutamate in bEND5 cells [51], as more widely illustrated below, and was indicative of receptor desensitization during the prolonged exposure to the agonist. Accordingly, the Ca²⁺ response to glutamate did not resume upon 15 min of washout. The following pieces of evidence indicate that glutamate-evoked Ca²⁺ signals in hCMEC/D3 cells are triggered by group 1 mGluRs. First, NMDARs-induced Ca²⁺ entry in microvascular endothelial cells cannot be elicited by physiological doses of glutamate, such as those employed in the present investigation [60, 61], in the absence of its co-agonists D-serine or glycine [49, 81]. Second, the Ca²⁺

response to glutamate arose in the absence of extracellular Ca²⁺, i.e., a condition which prevents NMDAR signaling [62], whereas G_qPCRs are still able to release endogenous Ca²⁺ in an InsP₃-dependent manner [51, 53]. Third, glutamate-induced increase in [Ca²⁺]_i was inhibited by MCPG and phenocopied by tACPD, which, respectively, inhibit [32, 51, 62] and activate [72] group 1 mGluRs. Fourth, mGluR1 and mGluR5 transcripts and proteins were expressed in hCMEC/D3 cells, as previously demonstrated in primary human microvascular endothelial cells [54] and in human cortical microvessels [55]. Moreover, pharmacological blockade of mGluR1 and mGluR5 with CPCCOEt and MTEP, respectively, impaired the Ca²⁺ response to glutamate, although only MTEP significantly reduced also the percentage of responding cells. In addition, the extent of inhibition of the Ca²⁺ response to glutamate by MTEP was larger as compared to CPCCOEt. These observations led us to conclude that mGluR1 and mGluR5 drive glutamate-induced elevation in [Ca²⁺]_i in hCMEC/D3 cells, although the contribution of mGluR5 is seemingly

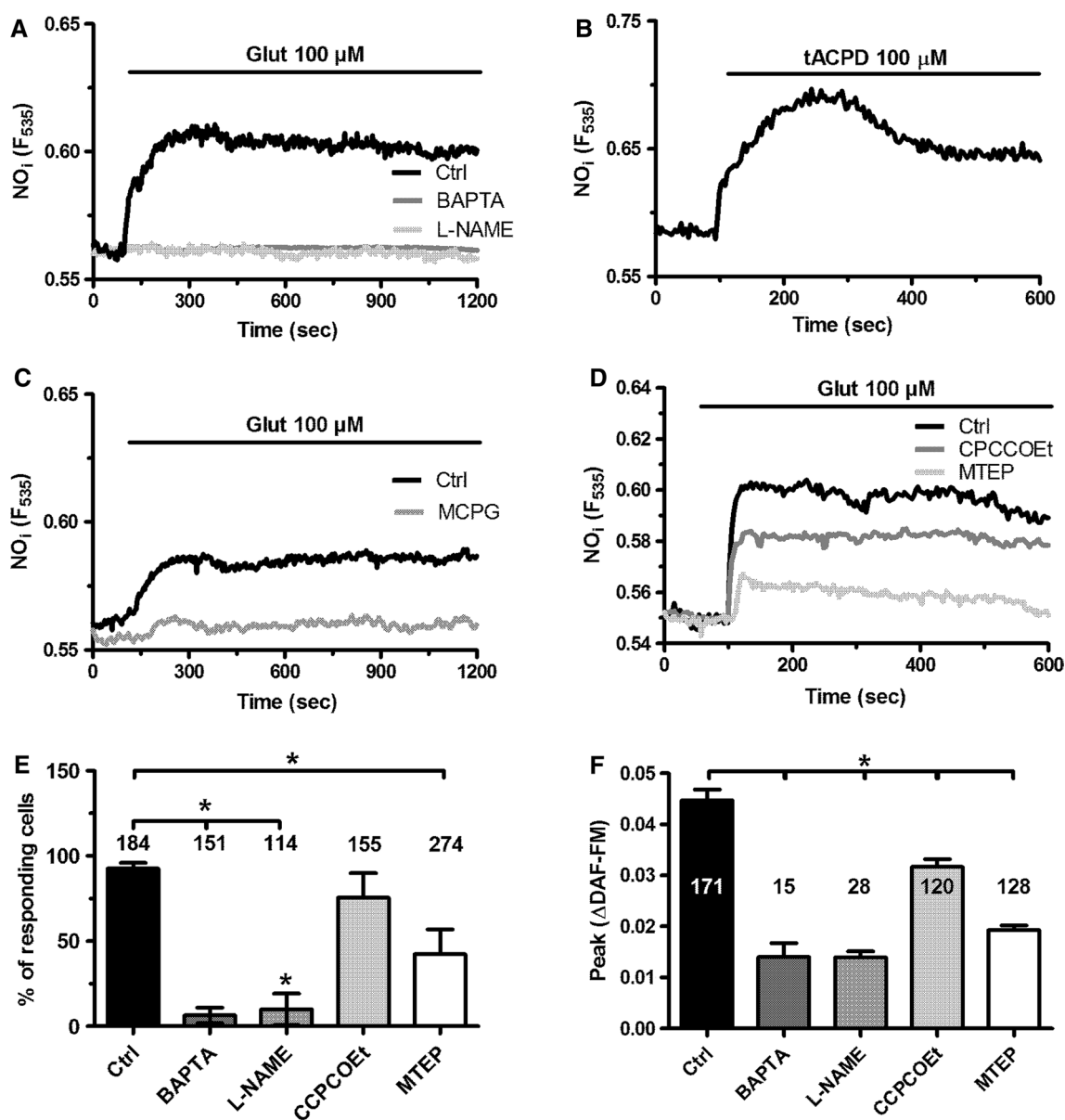


Fig. 7 Glutamate-induced NO release in hCMEC/D3 cells through the stimulation of mGluR1 and mGluR5. **a** Glutamate (100 μ M) caused a robust increase in DAF/FM fluorescence in hCMEC/D3 cells, that was strongly reduced by either L-NAME (100 μ M, 2 h), an inhibitor of NO synthase, or BAPTA (30 μ M, 2 h), a membrane-permeable intracellular Ca^{2+} chelator. **b** Glutamate induced a massive increase in NO production, which was inhibited by MCPG (150 μ M, 20 min). **c** *Trans*-ACPD (100 μ M) induced robust NO release in

hCMEC/D3 cells, thereby phenocopying the response to glutamate. **d** Glutamate-induced NO release was reduced by CCPCOEt (100 μ M, 10 min) and MTEP (100 μ M, 10 min). **e** Bar histogram shows the mean \pm SE of the percentage of responding cells under the designated treatments. The asterisk indicates $p < 0.05$ as compared to control cells. **f** Bar histogram shows the mean \pm SE of the amplitude of the response under the designated treatments. The asterisk indicates that $p < 0.05$ as compared to control cells

larger. Accordingly, specific mGluR5 activation with CHPG induced a Ca^{2+} signal in 100% of the recorded cells. Intriguingly, mGluR5 represents also the main isoform whereby glutamate triggers intracellular Ca^{2+} waves in rodent astrocytes both in vitro and in vivo [36, 63, 87]. Despite the fact that mGluR5 are less expressed as compared to mGluR1 transcripts in hCMEC/D3 cells, the finding that mGluR5 plays a pivotal role in the Ca^{2+} response to glutamate is not surprising.

Accordingly, it has long been known that, when mGluR1 and mGluR5 are co-expressed in brain neurons, mGluR1 induces lower PIP_2 hydrolysis, and, therefore, $InsP_3$ -dependent signaling, as compared to mGluR5 [88, 89]. In addition, recent work provided the evidence that only small clusters of $InsP_3$ Rs located beneath the plasma membrane are licensed to respond to extracellular stimuli [90]. One could speculate that most of these $InsP_3$ R clusters are packed in close proximity of mGluR5

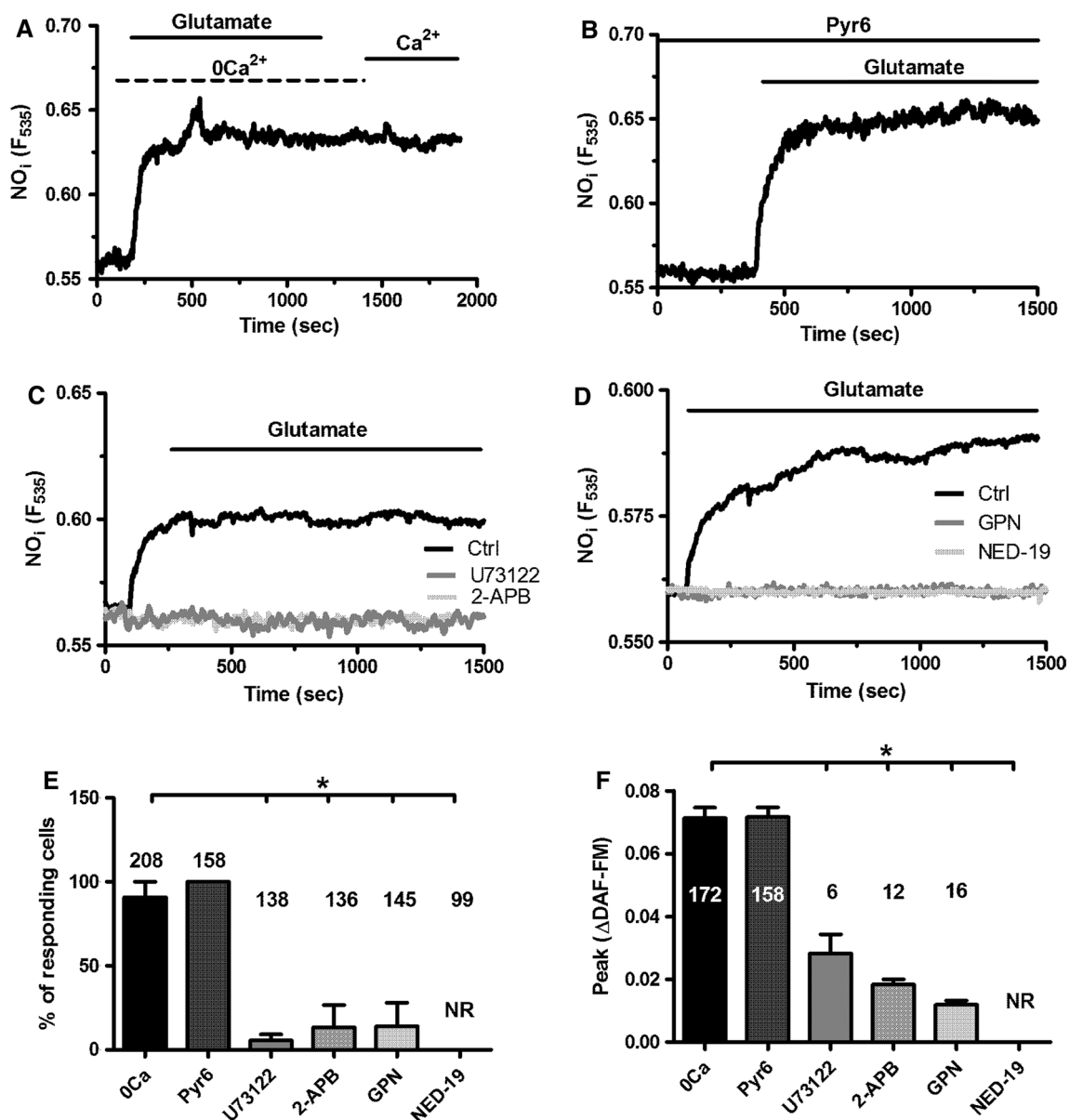


Fig. 8 Glutamate-induced intracellular Ca²⁺ signaling drives NO release in hCMEC/D3 cells. **a** Glutamate-induced NO release was not prevented by removal of extracellular Ca²⁺ (0Ca²⁺). Glutamate was administered at 100 μM. **b** Glutamate-induced NO release was not prevented by SOCE inhibition with Pyr6 (10 μM, 10 min). Glutamate was administered at 100 μM. **c** Glutamate-induced NO release was abolished by U73122 (10 μM, 30 min) and by 2-APB (50 μM, 30 min). Glutamate was administered at 100 μM. **d** Glutamate-

induced NO release was inhibited by GPN (200 μM) and NED-19 (100 μM, 30 min). Glutamate was administered at 100 μM. **e** Bar histogram shows the mean ± SE of the percentage of responding cells under the designated treatments. The asterisk indicates *p* < 0.05. **f** Bar histogram shows the mean ± SE of the amplitude of the response under the designated treatments. The asterisk indicates that *p* < 0.05. NR no response

rather than mGluR1 in hCMEC/D3 cells. Therefore, the desensitization of the Ca²⁺ signal occurring at higher doses of glutamate and during prolonged stimulation could be ascribed either to the prolonged phosphorylation of the intracellular COOH-terminus at position Ser839 of mGluR5 [91], which is the major receptor isoform involved in the onset of the signal, or the receptor internalization by G protein-coupled receptor kinase 2 [92], as observed in other brain cell types.

The role of InsP₃, NAADP, and SOCE in glutamate-induced Ca²⁺ signals

The following pieces of evidence indicate that the Ca²⁺ response to glutamate is supported by InsP₃- and NAADP-dependent intracellular Ca²⁺ release and prolonged by SOCE. First, glutamate-induced Ca²⁺ signals were abrogated by U73122, a selective PLC blocker, and by 2-APB, which

specifically targets InsP₃Rs under the conditions employed in the present investigation. Accordingly, the effect of 2-APB, which could also target Orai and TRP channels at 50 μM [67], has been probed upon removal of extracellular Ca²⁺, when extracellular Ca²⁺ entry cannot occur. InsP₃R3 presents the lowest affinity to InsP₃ and Ca²⁺ as compared to InsP₃R1 and InsP₃R2 and lacks the Ca²⁺-induced inhibition observed at high Ca²⁺ concentrations nearby the receptor [93, 94]. Therefore, InsP₃R3 functions as anti-oscillatory unit and maintains transient Ca²⁺ signatures [93, 94]. Conversely, bEND5 cells express InsP₃R1 and InsP₃R2, while they lack InsP₃R3: this subtle difference in the Ca²⁺ toolkit could explain why glutamate initiates long-last intracellular Ca²⁺ oscillations in this cell type [51]. Second, depletion of the ER Ca²⁺ pool with CPA fully suppressed the intracellular Ca²⁺ response to glutamate. Third, glutamate-induced increase in [Ca²⁺]_i was eradicated by depleting the EL Ca²⁺ pool with GPN and upon pharmacological blockade of TPC1-2 with NED-19. Notably, NAADP and InsP₃ interact to sustain the endogenous Ca²⁺ response to glutamate also in rodent hippocampal neurons [95] and astrocytes [96] and in mouse brain microvascular endothelial cells [51]. Moreover, NAADP and InsP₃ also cooperate to trigger acetylcholine-induced Ca²⁺ and NO release in hCMEC/D3 cells [53] and to trigger the endothelial Ca²⁺ activity induced by multiple agonists throughout the vascular bed [24, 97, 98]. According to the so-called “trigger hypothesis”, extracellular stimuli evoke NAADP-mediated spatially restricted EL Ca²⁺ signals which are then globalized into a cytosolic Ca²⁺ wave by the recruitment of juxtaposed InsP₃Rs through the Ca²⁺-induced Ca²⁺ release (CICR) process [76, 99]. RyRs, which are also engaged by NAADP-dependent EL Ca²⁺ release [99], are absent in hCMEC/D3 cells [53], and are not involved in the Ca²⁺ response to glutamate. The peak Ca²⁺ signal was not affected in the absence of extracellular Ca²⁺, although its duration was remarkably curtailed (see Fig. 2a, b). These effects were mimicked by Pyr6, thereby suggesting that SOCE was engaged by ER Ca²⁺ depletion to prolong glutamate-induced increase in [Ca²⁺]_i. The role of SOCE was further supported by the evidence that glutamate-induced extracellular Ca²⁺ entry was sensitive to BTP-2. Moreover, glutamate-induced extracellular Ca²⁺ entry could arise upon ER Ca²⁺ depletion and in the absence of the agonist from the bath, which suggests that Ca²⁺ influx does not require ligand or second messenger binding to the Ca²⁺ permeable pathway [64, 65]. We, therefore, hypothesize that SOCE prolongs the duration of the Ca²⁺ response to glutamate, as observed when hCMEC/D3 cells are challenged with acetylcholine [53] and in vascular endothelial cells upon G_qPCR stimulation [9, 11]. Our previous work provided the evidence that SOCE was mediated by STIM2 and Orai1 in hCMEC/D3 cells, as STIM1 was not expressed [53] and Pyr6 is regarded as a selective Orai1 blocker [66, 67]. Herein, we further showed that glutamate-evoked Ca²⁺ entry is sensitive to BTP-2, another established

Orai1 inhibitor [69, 71]. Indeed, although BTP-2 may also target TRPC5 [100], this channel is not expressed in hCMEC/D3 cells [14]. Previous work also showed that hCMEC/D3 cells express Orai2 and Orai3 [14]. However, Orai2 has been shown to serve as negative modulator of Orai1 in brain microvascular endothelial cells [15], a finding that has been confirmed also in mouse enamel cells [16] and T cells [17]. Moreover, a number of studies argued against the contribution of Orai3 to endothelial SOCE [11, 101, 102], as this Orai isoform has hitherto been implicated only in leukotriene C4-induced Ca²⁺ entry in vascular endothelial cells [103].

Glutamate-induced Ca²⁺ signals drive NO release in hCMEC/D3 cells

It has recently been shown that glutamate-induced metabolic Ca²⁺ oscillations promote NO release in bEND5 cells [18]. The present investigation revealed that mGluR1 and, at a larger extent, mGluR5 elicited NO release through NAADP- and InsP₃-induced intracellular Ca²⁺ signals also in hCMEC/D3 cells. Accordingly, glutamate-induced NO release was phenocopied by t-ACPD and suppressed by any of the following treatments: (1) unspecific inhibition of group 1 mGluRs with MCPG; (2) pharmacological blockade of mGluR1 and mGluR5 with CPCCOEt and MTEP, respectively; and (3) preventing the increase in [Ca²⁺]_i with BAPTA or through pharmacological blockade of the InsP₃- and NAADP-signaling pathways. Conversely, glutamate-induced NO release was not impaired by removal of extracellular Ca²⁺ or pharmacological blockade of SOCE, which suggests that SOCE does not drive eNOS recruitment. This finding was somehow unexpected as SOCE is routinely required to sustain NO production in vascular endothelial cells [9, 21], including mouse [56] and human [53] brain endothelial cells challenged with acetylcholine. It is, therefore, likely that the eNOS pool recruited by glutamate is physically closer to InsP₃R3 and TPC1-2 rather than Orai1 in hCMEC/D3 cells and is selectively engaged by endogenously released Ca²⁺. In vascular endothelial cells, the vast majority of eNOS is localized to plasma membrane caveolae [104], which are apposed to ER cisternae and could be easily invested by InsP₃-induced ER Ca²⁺ release [105]. As functionally different sources of eNOS exist in vascular endothelium [104, 106], it is conceivable that acetylcholine and glutamate impinge on two distinct eNOS pools, one that is regulated by Orai1 and a second pool that is activated by InsP₃R3.

The putative role of endothelial group 1 mGluRs in NVC

The following pieces of evidence recently hinted at an unexpected role of brain microvascular endothelial cells

in NVC [8, 27, 29]. First, the hemodynamic response to neuronal activity is often initiated by cortical capillaries, which are wrapped by contracting pericytes and deliver a retrograde vasorelaxing signal to upstream arterioles and pial arteries to irrigate the activated area [32, 38, 42, 80]. According to this model, brain microvascular endothelial cells are placed in the ideal position to sense neuronal activity and directly control CBF [8, 27, 29]. Second, discrete interruption of endothelial signaling dampens stimulus-evoked retrograde propagation of vasodilation in pial arteries, whereas wide-field disruption of the endothelial monolayer significantly attenuates the hemodynamic signal [107]. Third, activation of endothelial G_q PCRs by neuronal activity at capillary level was recently shown to modulate the onset and retrograde propagation of the hemodynamic signal in a Ca^{2+} -dependent manner [26]. These observations indicated that brain microvascular endothelial cells endowed with NMDARs, and/or mGluRs, were able to detect and react to synaptically released glutamate. Consistently, it was first shown that neuronal activity stimulated perisynaptic astrocytes to release D-serine, thereby inducing cortical arteriole vasodilation by activating endothelial NMDARs and recruiting eNOS in mouse

brain [49, 50, 81]. Subsequently, glutamate was found to induce metabotropic Ca^{2+} signals and NO release in mouse brain microvascular endothelial cells [51]. The findings reported in the present investigation lend further support to the notion that brain microvascular endothelium actively participates in NVC and suggest an alternative mechanism to understand the role played by group 1 mGluRs in functional hyperemia. Neuronal (and endothelial) ionotropic NMDARs trigger NVC by inducing fast NO release, which directly or indirectly elicits the rapid component of the vasorelaxing response [31–34, 81]. Endothelial mGluRs could in turn support the slower component of the hemodynamic signal during prolonged (up to 1 min) synaptic stimulation either by directly vasorelaxing mural cells (i.e., vascular smooth muscle cells and pericytes) or facilitating EETs-induced vasodilation [31, 33, 34]. The finding that group 1 mGluRs are expressed in brain microvascular endothelial cells and elicit Ca^{2+} -dependent NO release could help to understand the long known inhibitory effect of CPCCOEt and MTEP on NVC. Accordingly, although it has long been known that group 1 mGluRs somehow regulate NVC and drive the Ca^{2+} -dependent release of EETs from astrocytes, how this occurs is matter of controversy

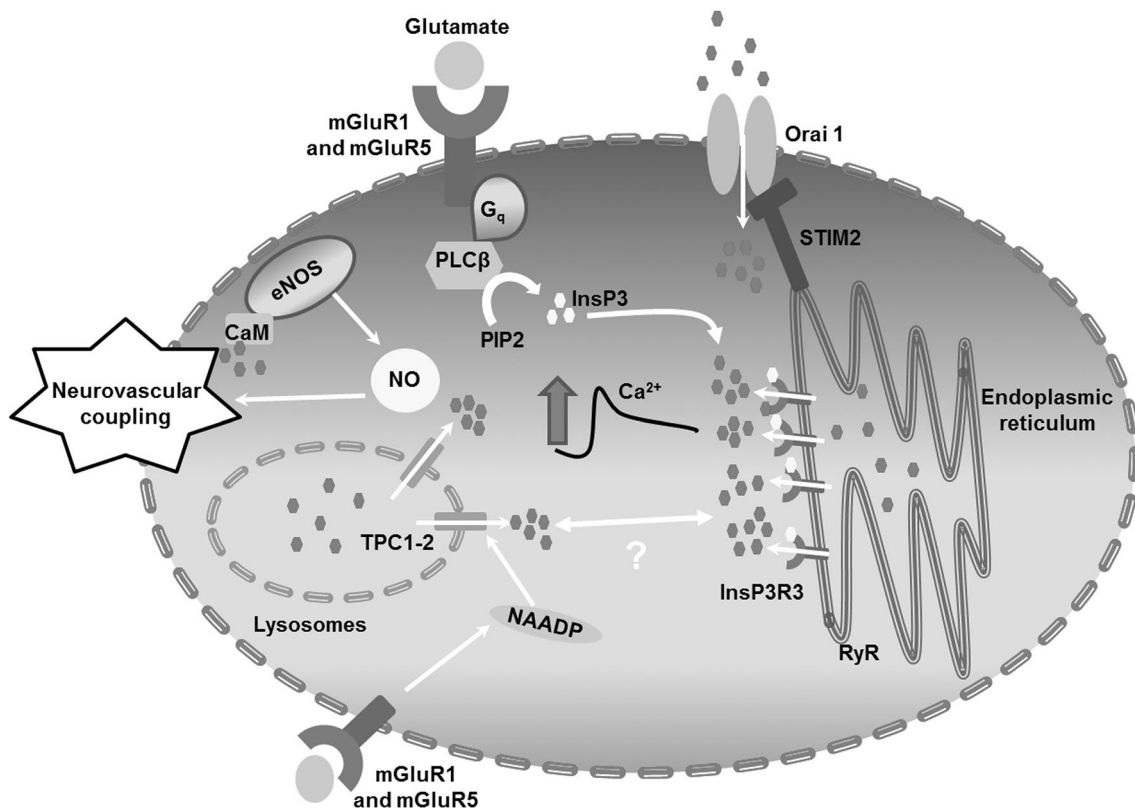


Fig. 9 Schematic representation of glutamate-induced Ca^{2+} and NO signals in hCMEC/D3 cells. The neurotransmitter glutamate binds to mGluR1 and mGluR5 to elicit an increase in $[\text{Ca}^{2+}]_i$ in hCMEC/D3 cells. The Ca^{2+} response to glutamate is patterned by InsP_3R_3 , TPC1-

2, and SOCE, and results in eNOS recruitment and NO release. NO, in turn, is predicted to regulate neurovascular coupling (NVC) within brain microcirculation

[39–42]. Notably, a recent study demonstrated that synaptic glutamate induces astrocytic Ca^{2+} signals and arteriolar vasodilation by inducing endothelial-dependent NO release in vivo [48]. Therefore, we hypothesize that the effect exerted by CPCCOeT and MTEP on NVC should rather be ascribed to its inhibitory action on endothelial group 1 mGluRs, which triggers robust NO production and could, therefore, be responsible for astrocyte activation and EET release. This hypothesis, however, remains to be experimentally probed and will be the focus of future investigation.

Conclusion

In conclusion, this investigation demonstrates for the first time that glutamate is able to induce Ca^{2+} -dependent NO release by selectively activating mGluR1 and mGluR5 in human brain microvascular endothelial cells. The Ca^{2+} response to glutamate is initiated by endogenous Ca^{2+} release through $\text{InsP}_3\text{R3}$ and NAADP-gated TPCs and sustained by SOCE (Fig. 9), although only endogenous Ca^{2+} mobilization drives NO production. These observations reinforce the view that the cellular and molecular mechanisms of NVC should be revisited by taking brain microvascular endothelial cells into account and propose an alternative model to explain the documented involvement of group 1 mGluRs in NVC.

Acknowledgements This research was funded by: Italian Ministry of Education, University and Research (MIUR): Dipartimenti di Eccellenza Program (2018–2022)—Dept. of Biology and Biotechnology “L. Spallanzani”, University of Pavia (F.M.), and by Fondo Ricerca Giovani from the University of Pavia (F.M.). P.S.F. was supported by MAECI (Ministero degli Affari Esteri e della Cooperazione Internazionale).

References

- McCarron JG, Lee MD, Wilson C (2017) The endothelium solves problems that endothelial cells do not know exist. *Trends Pharmacol Sci* 38(4):322–338. <https://doi.org/10.1016/j.tips.2017.01.008>
- Moccia F, Tanzi F, Munaron L (2014) Endothelial remodelling and intracellular calcium machinery. *Curr Mol Med* 14(4):457–480
- Khaddaj Mallat R, Mathew John C, Kendrick DJ, Braun AP (2017) The vascular endothelium: a regulator of arterial tone and interface for the immune system. *Crit Rev Clin Lab Sci* 54(7–8):458–470. <https://doi.org/10.1080/10408363.2017.1394267>
- Moccia F, Guerra G (2016) $\text{Ca}(2+)$ signalling in endothelial progenitor cells: friend or foe? *J Cell Physiol* 231(2):314–327. <https://doi.org/10.1002/jcp.25126>
- Kerr P, Tam R, Plane F (2011) Endothelium. In: Fitzridge R, Thompson M (eds) *Mechanisms of vascular disease: a reference book for vascular specialists*. University of Adelaide Press, Adelaide (AU)
- Godo S, Shimokawa H (2017) Endothelial functions. *Arterioscler Thromb Vasc Biol* 37(9):e108–e114. <https://doi.org/10.1161/ATVBAHA.117.309813>
- Garland CJ, Dora KA (2017) EDH: endothelium-dependent hyperpolarization and microvascular signalling. *Acta Physiol* 219(1):152–161. <https://doi.org/10.1111/apha.12649>
- Guerra G, Lucariello A, Perna A, Botta L, De Luca A, Moccia F (2018) The role of endothelial $\text{Ca}(2+)$ signaling in neurovascular coupling: a view from the Lumen. *Int J Mol Sci*. <https://doi.org/10.3390/ijms19040938>
- Blatter LA (2017) Tissue specificity: SOCE: implications for Ca^{2+} handling in endothelial cells. *Adv Exp Med Biol* 993:343–361. https://doi.org/10.1007/978-3-319-57732-6_18
- Moccia F, Dragoni S, Lodola F, Bonetti E, Bottino C, Guerra G et al (2012) Store-dependent $\text{Ca}(2+)$ entry in endothelial progenitor cells as a perspective tool to enhance cell-based therapy and adverse tumour vascularization. *Curr Med Chem* 19(34):5802–5818
- Abdullaev IF, Bisaillon JM, Potier M, Gonzalez JC, Motiani RK, Trebak M (2008) Stim1 and Orai1 mediate CRAC currents and store-operated calcium entry important for endothelial cell proliferation. *Circ Res* 103(11):1289–1299. <https://doi.org/10.1161/01.res.0000338496.95579.56>
- Li J, Cubbon RM, Wilson LA, Amer MS, McKeown L, Hou B et al (2011) Orai1 and CRAC channel dependence of VEGF-activated Ca^{2+} entry and endothelial tube formation. *Circ Res* 108(10):1190–1198. <https://doi.org/10.1161/circresaha.111.243352>
- Sachdeva R, Fleming T, Schumacher D, Homberg S, Stolz K, Mohr F et al (2019) Methylglyoxal evokes acute $\text{Ca}(2+)$ transients in distinct cell types and increases agonist-evoked $\text{Ca}(2+)$ entry in endothelial cells via CRAC channels. *Cell Calcium* 78:66–75. <https://doi.org/10.1016/j.ceca.2019.01.002>
- Zuccolo E, Laforenza U, Negri S, Botta L, Berra-Romani R, Faris P et al (2019) Muscarinic M5 receptors trigger acetylcholine-induced $\text{Ca}(2+)$ signals and nitric oxide release in human brain microvascular endothelial cells. *J Cell Physiol* 234(4):4540–4562. <https://doi.org/10.1002/jcp.27234>
- Kito H, Yamamura H, Suzuki Y, Yamamura H, Ohya S, Asai K et al (2015) Regulation of store-operated Ca^{2+} entry activity by cell cycle dependent up-regulation of Orai2 in brain capillary endothelial cells. *Biochem Biophys Res Commun* 459(3):457–462. <https://doi.org/10.1016/j.bbrc.2015.02.127>
- Eckstein M, Vaeth M, Aulestia FJ, Costiniti V, Kassam SN, Bromage TG et al (2019) Differential regulation of $\text{Ca}(2+)$ influx by ORAI channels mediates enamel mineralization. *Sci Signal*. <https://doi.org/10.1126/scisignal.aav4663>
- Vaeth M, Yang J, Yamashita M, Zee I, Eckstein M, Knosp C et al (2017) ORAI2 modulates store-operated calcium entry and T cell-mediated immunity. *Nat Commun* 8:14714. <https://doi.org/10.1038/ncomms14714>
- Zuccolo E, Kheder DA, Lim D, Perna A, Nezza FD, Botta L et al (2019) Glutamate triggers intracellular $\text{Ca}(2+)$ oscillations and nitric oxide release by inducing NAADP- and InsP_3 -dependent $\text{Ca}(2+)$ release in mouse brain endothelial cells. *J Cell Physiol* 234(4):3538–3554. <https://doi.org/10.1002/jcp.26953>
- Fukao M, Hattori Y, Kanno M, Sakuma I, Kitabatake A (1997) Sources of Ca^{2+} in relation to generation of acetylcholine-induced endothelium-dependent hyperpolarization in rat mesenteric artery. *Br J Pharmacol* 120(7):1328–1334. <https://doi.org/10.1038/sj.bjp.0701027>
- Freichel M, Suh SH, Pfeifer A, Schweig U, Trost C, Weissgerber P et al (2001) Lack of an endothelial store-operated Ca^{2+} current

- impairs agonist-dependent vasorelaxation in TRP4^{-/-} mice. *Nat Cell Biol* 3(2):121–127. <https://doi.org/10.1038/35055019>
21. Berra-Romani R, Avelino-Cruz JE, Raqeeb A, Della Corte A, Cinelli M, Montagnani S et al (2013) Ca(2+)-dependent nitric oxide release in the injured endothelium of excised rat aorta: a promising mechanism applying in vascular prosthetic devices in aging patients. *BMC Surg* 13(Suppl 2):S40. <https://doi.org/10.1186/1471-2482-13-S2-S40>
 22. Blatter LA, Taha Z, Mesaros S, Shacklock PS, Wier WG, Malinski T (1995) Simultaneous measurements of Ca²⁺ and nitric oxide in bradykinin-stimulated vascular endothelial cells. *Circ Res* 76(5):922–924
 23. Lantoiné F, Iouzalén L, Devynck MA, Millanvoye-Van Brussel E, David-Duflho M (1998) Nitric oxide production in human endothelial cells stimulated by histamine requires Ca²⁺ influx. *Biochem J* 330(Pt 2):695–699
 24. Brailoiu GC, Gurzu B, Gao X, Parkesh R, Aley PK, Trifa DI et al (2010) Acidic NAADP-sensitive calcium stores in the endothelium: agonist-specific recruitment and role in regulating blood pressure. *J Biol Chem* 285(48):37133–37137. <https://doi.org/10.1074/jbc.C110.169763>
 25. Toth P, Tarantini S, Davila A, Valcarcel-Ares MN, Tucsek Z, Varamini B et al (2015) Purinergic glio-endothelial coupling during neuronal activity: role of P2Y1 receptors and eNOS in functional hyperemia in the mouse somatosensory cortex. *Am J Physiol Heart Circ Physiol* 309(11):H1837–H1845. <https://doi.org/10.1152/ajpheart.00463.2015>
 26. Harraz OF, Longden TA, Hill-Eubanks D, Nelson MT (2018) PIP2 depletion promotes TRPV4 channel activity in mouse brain capillary endothelial cells. *eLife*. <https://doi.org/10.7554/eLife.38689>
 27. Iadecola C (2017) The neurovascular unit coming of age: a journey through neurovascular coupling in health and disease. *Neuron* 96(1):17–42. <https://doi.org/10.1016/j.neuron.2017.07.030>
 28. Attwell D, Buchan AM, Charpak S, Lauritzen M, Macvicar BA, Newman EA (2010) Glial and neuronal control of brain blood flow. *Nature* 468(7321):232–243. <https://doi.org/10.1038/nature09613>
 29. Hillman EM (2014) Coupling mechanism and significance of the BOLD signal: a status report. *Annu Rev Neurosci* 37:161–181. <https://doi.org/10.1146/annurev-neuro-071013-014111>
 30. Lourenco CF, Ledo A, Barbosa RM, Laranjinha J (2017) Neurovascular-neuroenergetic coupling axis in the brain: master regulation by nitric oxide and consequences in aging and neurodegeneration. *Free Radic Biol Med* 108:668–682. <https://doi.org/10.1016/j.freeradbiomed.2017.04.026>
 31. Lourenco CF, Santos RM, Barbosa RM, Cadenas E, Radi R, Laranjinha J (2014) Neurovascular coupling in hippocampus is mediated via diffusion by neuronal-derived nitric oxide. *Free Radic Biol Med* 73:421–429. <https://doi.org/10.1016/j.freeradbiomed.2014.05.021>
 32. Mapelli L, Gagliano G, Soda T, Laforenza U, Moccia F, D'Angelo EU (2017) Granular layer neurons control cerebellar neurovascular coupling through an NMDA receptor/NO-dependent system. *J Neurosci* 37(5):1340–1351. <https://doi.org/10.1523/JNEUROSCI.2025-16.2016>
 33. Cauli B, Hamel E (2010) Revisiting the role of neurons in neurovascular coupling. *Front Neuroenerg* 2:9. <https://doi.org/10.3389/fnene.2010.00009>
 34. Duchemin S, Boily M, Sadekova N, Girouard H (2012) The complex contribution of NOS interneurons in the physiology of cerebrovascular regulation. *Front Neural Circuits* 6:51. <https://doi.org/10.3389/fncir.2012.00051>
 35. Liu X, Li C, Falck JR, Roman RJ, Harder DR, Koehler RC (2008) Interaction of nitric oxide, 20-HETE, and EETs during functional hyperemia in whisker barrel cortex. *Am J Physiol Heart Circ Physiol* 295(2):H619–H631. <https://doi.org/10.1152/ajpheart.01211.2007>
 36. Zonta M, Angulo MC, Gobbo S, Rosengarten B, Hossmann KA, Pozzan T et al (2003) Neuron-to-astrocyte signaling is central to the dynamic control of brain microcirculation. *Nat Neurosci* 6(1):43–50. <https://doi.org/10.1038/mn980>
 37. Mulligan SJ, MacVicar BA (2004) Calcium transients in astrocyte endfeet cause cerebrovascular constrictions. *Nature* 431(7005):195–199. <https://doi.org/10.1038/nature02827>
 38. Hall CN, Reynell C, Gesslein B, Hamilton NB, Mishra A, Sutherland BA et al (2014) Capillary pericytes regulate cerebral blood flow in health and disease. *Nature* 508(7494):55–60. <https://doi.org/10.1038/nature13165>
 39. Lecrux C, Toussay X, Kocharyan A, Fernandes P, Neupane S, Levesque M et al (2011) Pyramidal neurons are “neurogenic hubs” in the neurovascular coupling response to whisker stimulation. *J Neurosci* 31(27):9836–9847. <https://doi.org/10.1523/JNEUROSCI.4943-10.2011>
 40. Sloan HL, Austin VC, Blamire AM, Schnupp JW, Lowe AS, Allers KA et al (2010) Regional differences in neurovascular coupling in rat brain as determined by fMRI and electrophysiology. *Neuroimage* 53(2):399–411. <https://doi.org/10.1016/j.neuroimage.2010.07.014>
 41. Shi Y, Liu X, Gebremedhin D, Falck JR, Harder DR, Koehler RC (2008) Interaction of mechanisms involving epoxyeicosatrienoic acids, adenosine receptors, and metabotropic glutamate receptors in neurovascular coupling in rat whisker barrel cortex. *J Cereb Blood Flow Metab* 28(1):111–125. <https://doi.org/10.1038/sj.jcbfm.9600511>
 42. Rungta RL, Chaigneau E, Osmanski BF, Charpak S (2018) Vascular Compartmentalization of Functional Hyperemia from the Synapse to the Pia. *Neuron*. 99(2):362–375. <https://doi.org/10.1016/j.neuron.2018.06.012>
 43. Cauli B, Hamel E (2018) Brain perfusion and astrocytes. *Trends Neurosci* 41(7):409–413. <https://doi.org/10.1016/j.tins.2018.04.010>
 44. Nortley R, Attwell D (2017) Control of brain energy supply by astrocytes. *Curr Opin Neurobiol* 47:80–85. <https://doi.org/10.1016/j.conb.2017.09.012>
 45. Kisler K, Nelson AR, Montagne A, Zlokovic BV (2017) Cerebral blood flow regulation and neurovascular dysfunction in Alzheimer disease. *Nat Rev Neurosci* 18(7):419–434. <https://doi.org/10.1038/nrn.2017.48>
 46. Lecrux C, Hamel E (2016) Neuronal networks and mediators of cortical neurovascular coupling responses in normal and altered brain states. *Philos Trans R Soc Lond B Biol Sci*. <https://doi.org/10.1098/rstb.2015.0350>
 47. Niswender CM, Conn PJ (2010) Metabotropic glutamate receptors: physiology, pharmacology, and disease. *Annu Rev Pharmacol Toxicol* 50:295–322. <https://doi.org/10.1146/annurev.pharmtox.011008.145533>
 48. Tran CHT, Peringod G, Gordon GR (2018) Astrocytes integrate behavioral state and vascular signals during functional hyperemia. *Neuron* 100(5):1133–1148. <https://doi.org/10.1016/j.neuron.2018.09.045>
 49. LeMaistre JL, Sanders SA, Stobart MJ, Lu L, Knox JD, Anderson HD et al (2012) Coactivation of NMDA receptors by glutamate and D-serine induces dilation of isolated middle cerebral arteries. *J Cereb Blood Flow Metab* 32(3):537–547. <https://doi.org/10.1038/jcbfm.2011.161>
 50. Lu L, Hogan-Cann AD, Globa AK, Lu P, Nagy JJ, Bamji SX et al (2017) Astrocytes drive cortical vasodilatory signaling by activating endothelial NMDA receptors. *J Cereb Blood Flow Metab*. <https://doi.org/10.1177/0271678x17734100>
 51. Zuccolo E, Kheder DA, Lim D, Perna A, Nezza FD, Botta L et al (2018) Glutamate triggers intracellular Ca(2+)

- oscillations and nitric oxide release by inducing NAADP- and InsP3-dependent Ca(2+) release in mouse brain endothelial cells. *J Cell Physiol*. <https://doi.org/10.1002/jcp.26953>
52. Hopper RA, Garthwaite J (2006) Tonic and phasic nitric oxide signals in hippocampal long-term potentiation. *J Neurosci* 26(45):11513–11521. <https://doi.org/10.1523/JNEUROSCI.2259-06.2006>
 53. Zuccolo E, Laforenza U, Negri S, Botta L, Berra-Romani R, Faris P et al (2018) Muscarinic M5 receptors trigger acetylcholine-induced Ca(2+) signals and nitric oxide release in human brain microvascular endothelial cells. *J Cell Physiol*. <https://doi.org/10.1002/jcp.27234>
 54. Collard CD, Park KA, Montalto MC, Alapati S, Buras JA, Stahl GL et al (2002) Neutrophil-derived glutamate regulates vascular endothelial barrier function. *J Biol Chem* 277(17):14801–14811. <https://doi.org/10.1074/jbc.M110557200>
 55. Gillard SE, Tzaferis J, Tsui HC, Kingston AE (2003) Expression of metabotropic glutamate receptors in rat meningeal and brain microvasculature and choroid plexus. *J Comp Neurol* 461(3):317–332. <https://doi.org/10.1002/cne.10671>
 56. Zuccolo E, Lim D, Kheder DA, Perna A, Catarsi P, Botta L et al (2017) Acetylcholine induces intracellular Ca²⁺ oscillations and nitric oxide release in mouse brain endothelial cells. *Cell Calcium* 66:33–47. <https://doi.org/10.1016/j.ceca.2017.06.003>
 57. Bootman MD, Rietdorf K, Collins T, Walker S, Sanderson M (2013) Ca²⁺-sensitive fluorescent dyes and intracellular Ca²⁺ imaging. *Cold Spring Harbor Protoc* 2013(2):83–99. <https://doi.org/10.1101/pdb.top066050>
 58. Yeung YG, Stanley ER (2009) A solution for stripping antibodies from polyvinylidene fluoride immunoblots for multiple reprobing. *Anal Biochem* 389(1):89–91
 59. Bradford MM (1976) A rapid and sensitive method for the quantitation of microgram quantities of protein utilizing the principle of protein-dye binding. *Anal Biochem* 72:248–254
 60. Clements JD, Lester RA, Tong G, Jahr CE, Westbrook GL (1992) The time course of glutamate in the synaptic cleft. *Science* 258(5087):1498–1501
 61. Lee KH, Kristic K, van Hoff R, Hitti FL, Blaha C, Harris B et al (2007) High-frequency stimulation of the subthalamic nucleus increases glutamate in the subthalamic nucleus of rats as demonstrated by in vivo enzyme-linked glutamate sensor. *Brain Res* 1162:121–129. <https://doi.org/10.1016/j.brainres.2007.06.021>
 62. Lim D, Mapelli L, Canonico PL, Moccia F, Genazzani AA (2018) Neuronal activity-dependent activation of astroglial calcineurin in mouse primary hippocampal cultures. *Int J Mol Sci*. <https://doi.org/10.3390/ijms19102997>
 63. Lim D, Iyer A, Ronco V, Grolla AA, Canonico PL, Aronica E et al (2013) Amyloid beta deregulates astroglial mGluR5-mediated calcium signaling via calcineurin and Nf-kB. *Glia* 61(7):1134–1145. <https://doi.org/10.1002/glia.22502>
 64. Sanchez-Hernandez Y, Laforenza U, Bonetti E, Fontana J, Dragoni S, Russo M et al (2010) Store-operated Ca(2+) entry is expressed in human endothelial progenitor cells. *Stem Cells Dev* 19(12):1967–1981. <https://doi.org/10.1089/scd.2010.0047>
 65. Bird GS, DeHaven WI, Smyth JT, Putney JW Jr (2008) Methods for studying store-operated calcium entry. *Methods* 46(3):204–212. <https://doi.org/10.1016/j.ymeth.2008.09.009>
 66. Schleifer H, Doleschal B, Lichtenegger M, Oppenrieder R, Derler I, Frischauf I et al (2012) Novel pyrazole compounds for pharmacological discrimination between receptor-operated and store-operated Ca(2+) entry pathways. *Br J Pharmacol* 167(8):1712–1722. <https://doi.org/10.1111/j.1476-5381.2012.02126.x>
 67. Prakriya M, Lewis RS (2015) Store-operated calcium channels. *Physiol Rev* 95(4):1383–1436. <https://doi.org/10.1152/physrev.00020.2014>
 68. Moccia F, Zuccolo E, Poletto V, Turin I, Guerra G, Pedrazzoli P et al (2016) Targeting stim and orai proteins as an alternative approach in anticancer therapy. *Curr Med Chem* 23(30):3450–3480
 69. Azimi I, Bong AH, Poo GXH, Armitage K, Lok D, Roberts-Thomson SJ et al (2018) Pharmacological inhibition of store-operated calcium entry in MDA-MB-468 basal A breast cancer cells: consequences on calcium signalling, cell migration and proliferation. *Cell Mol Life Sci* 75(24):4525–4537. <https://doi.org/10.1007/s00018-018-2904-y>
 70. Majeed Y, Amer MS, Agarwal AK, McKeown L, Porter KE, O'Regan DJ et al (2011) Stereo-selective inhibition of transient receptor potential TRPC5 cation channels by neuroactive steroids. *Br J Pharmacol* 162(7):1509–1520. <https://doi.org/10.1111/j.1476-5381.2010.01136.x>
 71. Zitt C, Strauss B, Schwarz EC, Spaeth N, Rast G, Hatzelmann A et al (2004) Potent inhibition of Ca²⁺ release-activated Ca²⁺ channels and T-lymphocyte activation by the pyrazole derivative BTP2. *J Biol Chem* 279(13):12427–12437. <https://doi.org/10.1074/jbc.M309297200>
 72. Filosa JA, Bonev AD, Nelson MT (2004) Calcium dynamics in cortical astrocytes and arterioles during neurovascular coupling. *Circ Res* 95(10):e73–e81. <https://doi.org/10.1161/01.RES.0000148636.60732.2e>
 73. Le Duigou C, Kullmann DM (2011) Group I mGluR agonist-evoked long-term potentiation in hippocampal oriens interneurons. *J Neurosci* 31(15):5777–5781. <https://doi.org/10.1523/JNEUROSCI.6265-10.2011>
 74. Kotova PD, Bystrova MF, Rogachevskaja OA, Khokhlov AA, Syssoeva VY, Tkachuk VA et al (2018) Coupling of P2Y receptors to Ca(2+) mobilization in mesenchymal stromal cells from the human adipose tissue. *Cell Calcium* 71:1–14. <https://doi.org/10.1016/j.ceca.2017.11.001>
 75. Cardenas C, Liberona JL, Molgo J, Colasante C, Mignery GA, Jaimovich E (2005) Nuclear inositol 1,4,5-trisphosphate receptors regulate local Ca²⁺ transients and modulate cAMP response element binding protein phosphorylation. *J Cell Sci* 118(Pt 14):3131–3140. <https://doi.org/10.1242/jcs.02446>
 76. Faris P, Shekha M, Montagna D, Guerra G, Moccia F (2018) Endolysosomal Ca(2+) signalling and cancer hallmarks: two-pore channels on the move, TRPML1 Lags Behind! *Cancers (Basel)*. <https://doi.org/10.3390/cancers11010027>
 77. Ronco V, Potenza DM, Denti F, Vullo S, Gagliano G, Tognolina M et al (2015) A novel Ca(2+)-mediated cross-talk between endoplasmic reticulum and acidic organelles: implications for NAADP-dependent Ca(2+)-signalling. *Cell Calcium* 57(2):89–100. <https://doi.org/10.1016/j.ceca.2015.01.001>
 78. Di Nezza F, Zuccolo E, Poletto V, Rosti V, De Luca A, Moccia F et al (2017) Liposomes as a putative tool to investigate NAADP signaling in vasculogenesis. *J Cell Biochem*. <https://doi.org/10.1002/jcb.26019>
 79. Pitt SJ, Reilly-O'Donnell B, Sitsapesan R (2016) Exploring the biophysical evidence that mammalian two-pore channels are NAADP-activated calcium-permeable channels. *J Physiol* 594(15):4171–4179. <https://doi.org/10.1113/JP270936>
 80. Longden TA, Dabertrand F, Koide M, Gonzales AL, Tykocki NR, Brayden JE et al (2017) Capillary K(+) sensing initiates retrograde hyperpolarization to increase local cerebral blood flow. *Nat Neurosci* 20(5):717–726. <https://doi.org/10.1038/nn.4533>
 81. Stobart JL, Lu L, Anderson HD, Mori H, Anderson CM (2013) Astrocyte-induced cortical vasodilation is mediated by D-serine and endothelial nitric oxide synthase. *Proc Natl Acad Sci USA* 110(8):3149–3154. <https://doi.org/10.1073/pnas.1215929110>
 82. Moccia F, Berra-Romani R, Tanzi F (2012) Update on vascular endothelial Ca²⁺ signalling: a tale of ion channels, pumps

- and transporters. *World J Biol Chem* 3(7):127–158. <https://doi.org/10.4331/wjbc.v3.i7.127>
83. Re F, Cambianica I, Sesana S, Salvati E, Cagnotto A, Salmons M et al (2011) Functionalization with ApoE-derived peptides enhances the interaction with brain capillary endothelial cells of nanoliposomes binding amyloid-beta peptide. *J Biotechnol* 156(4):341–346. <https://doi.org/10.1016/j.jbiotec.2011.06.037>
 84. Salvati E, Re F, Sesana S, Cambianica I, Sancini G, Masserini M et al (2013) Liposomes functionalized to overcome the blood–brain barrier and to target amyloid-beta peptide: the chemical design affects the permeability across an in vitro model. *Int J Nanomed* 8:1749–1758. <https://doi.org/10.2147/IJN.S42783>
 85. Veszelka S, Toth A, Walter FR, Toth AE, Grof I, Meszaros M et al (2018) Comparison of a rat primary cell-based blood–brain barrier model with epithelial and brain endothelial cell lines: gene expression and drug transport. *Front Mol Neurosci* 11:166. <https://doi.org/10.3389/fnmol.2018.00166>
 86. Bader A, Bintig W, Begandt D, Klett A, Siller IG, Gregor C et al (2017) Adenosine receptors regulate gap junction coupling of the human cerebral microvascular endothelial cells hCMEC/D3 by Ca(2+) influx through cyclic nucleotide-gated channels. *J Physiol* 595(8):2497–2517. <https://doi.org/10.1113/JP273150>
 87. Lind BL, Brazhe AR, Jessen SB, Tan FC, Lauritzen MJ (2013) Rapid stimulus-evoked astrocyte Ca²⁺ elevations and hemodynamic responses in mouse somatosensory cortex in vivo. *Proc Natl Acad Sci USA* 110(48):E4678–E4687. <https://doi.org/10.1073/pnas.1310065110>
 88. Casabona G, Knopfel T, Kuhn R, Gasparini F, Baumann P, Sortino MA et al (1997) Expression and coupling to polyphosphoinositide hydrolysis of group I metabotropic glutamate receptors in early postnatal and adult rat brain. *Eur J Neurosci* 9(1):12–17
 89. Kettunen P, Krieger P, Hess D, El Manira A (2002) Signaling mechanisms of metabotropic glutamate receptor 5 subtype and its endogenous role in a locomotor network. *J Neurosci* 22(5):1868–1873
 90. Thillaiappan NB, Chavda AP, Tovey SC, Prole DL, Taylor CW (2017) Ca(2+) signals initiate at immobile IP3 receptors adjacent to ER-plasma membrane junctions. *Nat Commun* 8(1):1505. <https://doi.org/10.1038/s41467-017-01644-8>
 91. Kim CH, Braud S, Isaac JT, Roche KW (2005) Protein kinase C phosphorylation of the metabotropic glutamate receptor mGluR5 on Serine 839 regulates Ca²⁺ oscillations. *J Biol Chem* 280(27):25409–25415. <https://doi.org/10.1074/jbc.M502644200>
 92. Ribeiro FM, Ferreira LT, Paquet M, Cregan T, Ding Q, Gros R et al (2009) Phosphorylation-independent regulation of metabotropic glutamate receptor 5 desensitization and internalization by G protein-coupled receptor kinase 2 in neurons. *J Biol Chem* 284(35):23444–23453. <https://doi.org/10.1074/jbc.M109.000778>
 93. Foskett JK, White C, Cheung KH, Mak DO (2007) Inositol trisphosphate receptor Ca²⁺ release channels. *Physiol Rev* 87(2):593–658. <https://doi.org/10.1152/physrev.00035.2006>
 94. Miyakawa T, Maeda A, Yamazawa T, Hirose K, Kurosaki T, Iino M (1999) Encoding of Ca²⁺ signals by differential expression of IP3 receptor subtypes. *EMBO J* 18(5):1303–1308. <https://doi.org/10.1093/emboj/18.5.1303>
 95. Foster WJ, Taylor HBC, Padamsey Z, Jeans AF, Galione A, Emptage NJ (2018) Hippocampal mGluR1-dependent long-term potentiation requires NAADP-mediated acidic store Ca(2+) signaling. *Sci Signal*. <https://doi.org/10.1126/scisignal.aat9093>
 96. Pereira GJ, Antonioli M, Hirata H, Ureshino RP, Nascimento AR, Bincoletto C et al (2017) Glutamate induces autophagy via the two-pore channels in neural cells. *Oncotarget* 8(8):12730–12740. <https://doi.org/10.18632/oncotarget.14404>
 97. Favia A, Desideri M, Gambarà G, D'Alessio A, Ruas M, Esposito B et al (2014) VEGF-induced neoangiogenesis is mediated by NAADP and two-pore channel-2-dependent Ca²⁺ signaling. *Proc Natl Acad Sci USA* 111(44):E4706–E4715. <https://doi.org/10.1073/pnas.1406029111>
 98. Zuccolo E, Dragoni S, Poletto V, Catarsi P, Guido D, Rappa A et al (2016) Arachidonic acid-evoked Ca²⁺ signals promote nitric oxide release and proliferation in human endothelial colony forming cells. *Vasc Pharmacol* 87:159–171. <https://doi.org/10.1016/j.vph.2016.09.005>
 99. Galione A (2015) A primer of NAADP-mediated Ca(2+) signaling: from sea urchin eggs to mammalian cells. *Cell Calcium* 58(1):27–47. <https://doi.org/10.1016/j.ceca.2014.09.010>
 100. He LP, Hewavitharana T, Soboloff J, Spassova MA, Gill DL (2005) A functional link between store-operated and TRPC channels revealed by the 3,5-bis(trifluoromethyl)pyrazole derivative, BTP2. *J Biol Chem* 280(12):10997–11006. <https://doi.org/10.1074/jbc.M411797200>
 101. Zhou MH, Zheng H, Si H, Jin Y, Peng JM, He L et al (2014) Stromal interaction molecule 1 (STIM1) and Orai1 mediate histamine-evoked calcium entry and nuclear factor of activated T-cells (NFAT) signaling in human umbilical vein endothelial cells. *J Biol Chem* 289(42):29446–29456. <https://doi.org/10.1074/jbc.M114.578492>
 102. Sundivakkam PC, Freichel M, Singh V, Yuan JP, Vogel SM, Flockerzi V et al (2012) The Ca(2+) sensor stromal interaction molecule 1 (STIM1) is necessary and sufficient for the store-operated Ca(2+) entry function of transient receptor potential canonical (TRPC) 1 and 4 channels in endothelial cells. *Mol Pharmacol* 81(4):510–526. <https://doi.org/10.1124/mol.111.074658>
 103. Li J, Bruns AF, Hou B, Rode B, Webster PJ, Bailey MA et al (2015) Orai3 surface accumulation and calcium entry evoked by vascular endothelial growth factor. *Arterioscler Thromb Vasc Biol* 35(9):1987–1994. <https://doi.org/10.1161/ATVBAHA.115.305969>
 104. Shu X, Keller TCT, Begandt D, Butcher JT, Biwer L, Keller AS et al (2015) Endothelial nitric oxide synthase in the microcirculation. *Cell Mol Life Sci* 72(23):4561–4575. <https://doi.org/10.1007/s00018-015-2021-0>
 105. Bundgaard M (1991) The three-dimensional organization of smooth endoplasmic reticulum in capillary endothelia: its possible role in regulation of free cytosolic calcium. *J Struct Biol* 107(1):76–85
 106. Biwer LA, Taddeo EP, Kenwood BM, Hoehn KL, Straub AC, Isakson BE (2016) Two functionally distinct pools of eNOS in endothelium are facilitated by myoendothelial junction lipid composition. *Biochim Biophys Acta* 1861(7):671–679. <https://doi.org/10.1016/j.bbalip.2016.04.014>
 107. Chen BR, Kozberg MG, Bouchard MB, Shaik MA, Hillman EM (2014) A critical role for the vascular endothelium in functional neurovascular coupling in the brain. *J Am Heart Assoc* 3(3):e000787. <https://doi.org/10.1161/JAHA.114.000787>

Publisher's Note Springer Nature remains neutral with regard to jurisdictional claims in published maps and institutional affiliations.